Investigating Solid-State Nuclear Magnetic Resonance as an analytical technique for measuring the biodegradability of polymers and biopolymers in compost.

By

James Anderson

A Master's Thesis

Submitted to the Department of Chemistry

Lancaster University

In Fulfilment of the Requirements

For a Master's Degree

April 2025

Abstract

The increasing use of biodegradable polymers in consumer and agricultural applications necessitates robust analytical techniques to assess their environmental degradation. This study investigates the utility of Solid-State Nuclear Magnetic Resonance (SSNMR) spectroscopy as a non-destructive, molecular-level tool for measuring the biodegradability of polymers and biopolymers in compost. Using ^{13}C CP-MAS NMR, we analyse relaxation dynamics and spectral evolution of materials such as PLA, PBAT/PBST, polyethylene, and starch-based plastics under composting conditions. T_1 relaxation profiling reveals distinct differences in molecular mobility and rigidity, with compost exhibiting rapid relaxation due to its hydrated, amorphous nature, while polymers like PE and starch plastics show slower relaxation indicative of structural persistence. Even at low polymer concentrations (e.g., 1:99 PLA: compost), characteristic signals remain detectable, demonstrating SSNMR's sensitivity to rigid molecular environments despite spectral interference from compost. Additionally, the impact of changeable variables such as pH and moisture is explored, showing that alkaline, wet compost significantly broadens spectral lines and reduces resolution due to increased molecular disorder and hydrolysis.

Acknowledgments

I would like to thank my supervisor, Professor David A Middleton for bringing his insightful expertise and experience to this project. His help and support have really helped me complete this paper and this degree. I would also like to thank the members of David's team who have acted like mentors to me whilst I complete this degree, so Liam Beckitt and Sophie Rawnsley-Lau thank you very much for your support.

I would also like to thank the entirety of Lancaster University for their support throughout my degree, both undergraduate and postgraduate. All the staff in the chemistry department are very helpful, and I have learnt so much from my time here.

I also acknowledge the undeniable help I received from the companies who sent me some of their polymers for me to do my research on, I am incredibly grateful for your cooperation so to Alpla, Oil Refineries LTD and Bioapply thank you. Special thanks to Saoirse Kathryn McConnell from Bioapply who was exceptionally helpful and took time out of he

busy schedule to have multiple video calls just to talk about my project which was amazing.

Finally, I want to thank my friends and family for their continued support throughout this last 18 months. Without their consistent support I would not have this paper completed and it is thanks to them that I was able to finish this project.

Table of Contents

List of Figures

List of Tables

List of Abbreviations

- SSNMR – Solid-State Nuclear Magnetic Resonance
- Mt – Metric tonnes
- PE – Polyethylene
- PP – Polypropylene
- PLA – Polylactic Acid
- TPS – Thermoplastic Starch
- FTIR – Fourier-Transform Infrared Spectroscopy
- Pyrolysis-GC/MS – Pyrolysis Gas Chromatography / Mass Spectroscopy
- PBAT – Polybutylene Adipate Terephthalate
- PBST – Polybutylene Succinate Terephthalate
- LDPE – Low-Density
- HDPE – High-Density

1. Project Overview

1.1 Research Aim

The primary research aim of this project was to evaluate the effectiveness of ^{13}Cdetected solid-state nuclear magnetic resonance (SSNMR) spectroscopy for detecting microplastics in compost. If successful, SSNMR could be used to monitor the time-dependent degradation of plastics in different soil environments and conditions.

1.2 Problem Statement

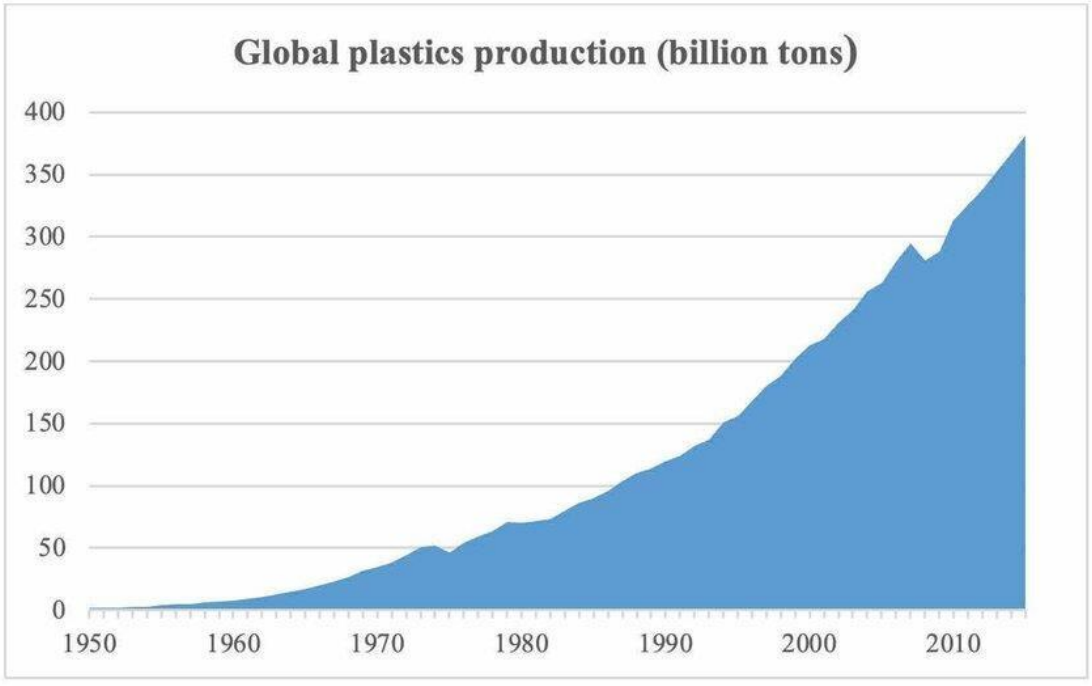

Figure 1. Global plastic production from 1950 to 2015.

The figure illustrates the continuous rise in global plastic production over the past 65 years, highlighting the corresponding increase in plastic waste generation associated with this growth (Statista Research Department, 2025).

In the past 50 years, global plastic production has surged 20-fold (Walker & Fequet, 2023), with an estimated of 9200 million metric tonnes (Mt) of plastic having been produced and more than 6900 Mt has been landfilled (Geyer et al., 2017) (Figure 1). As a result, plastic pollution is a growing issue for the environment and for human health.

This rapid increase reflects how reliant we are on plastics in every aspect of modern life, from packaging to medicine to electronics. However, despite this widespread use of plastics, we are failing to efficiently manage them after their lifecycle is over or they have completed the task for which they were designed.

Figure 2. Variety of microplastics in soil.

The figure illustrates the presence of microplastics within soil and compost environments, highlighting the range of particle types that can accumulate in terrestrial systems. (Morrison, 2024)

The amount of plastic that is recycled remains extremely low, with only 9% of all plastic produced worldwide being recycled (Geyer et al., 2017) , whilst 79% ends up in landfills or simply gets left to pollute different environments (Jambeck et al., 2015).This inefficient waste management is causing a build-up of plastic in the environment, with much of it breaking down into microplastics. These tiny particles, less than 5

millimetres in size (Hale et al., 2020), are often invisible to the naked eye, but can turn up anywhere – from deep-sea trenches to topsoil.

As the quantity of microplastics continues to grow, the more environments they end up occupying. This continuous growth increases the chances microplastics start entering our food chain and ending up in our bodies, causing damage to those most vulnerable. Microplastics have been found in breast milk (Caba-Flores et al., 2023) and even in infants' stools (Liu et al., 2023), only exemplifying how present microplastics are in every aspect of life. The toxicity present in these products can cause inflammation, immune disorders or even cancer in those most susceptible (Prata et al., 2020) so the problem cannot be understated.

This all adds to the urgency for efficient and reliable detection and subsequent reduction of microplastics in our environment, including in soil and compost. The requirement for analytical techniques that aid in the detection of microplastics in specific environments only increases as plastic production ramps up (Wirnkor et al., 2019) and the management of used plastics becomes more important. Being able to detect plastics in compost and learn how they interact over a period of time, experiments can be done determine what conditions are the most efficient to boost degradation, allowing prevention of plastics settling in such environments and removing them from the ecosystem.

Solid-state NMR (SSNMR) is potentially useful for detecting and characterising plastics in a variety of substrates, including soil and compost, because it can be used with minimal sample pre-treatment and provides atomic-level chemical information that can report on the rate and products of plastic degradation.

1.3 Research Objectives

The primary research objectives for this are:

- To test how well SSNMR can identify common non-biodegradable plastics like polyethylene (PE) and polypropylene (PP) (Cantor & Watts, 2011; Rani, 2024)
- To understand whether the technique can also detect biodegradable plastics like polylactic acid (PLA) and thermoplastic starch-based (TPS) materials (Khan et al., 2017).
- To explore the sensitivity of SSNMR to any chemical changes occurring in plastics as they degrade over time in a soil substrate.

- To examine whether changes in compost pH influences degradation and whether those changes are visible in the NMR spectra.

2. Introduction

2.1 The Growing Problem of Plastic Pollution

Recent studies estimate that around 4.8 to 12.7 million tonnes of plastic enter our oceans every year, and a large portion of this is eventually fragmented into microplastics (Jambeck et al., 2015). These small particles pose a significant threat because, due to their size, they are capable of infiltrating ecosystems in ways that larger plastic items cannot. Microplastics can absorb and concentrate toxic chemicals from their

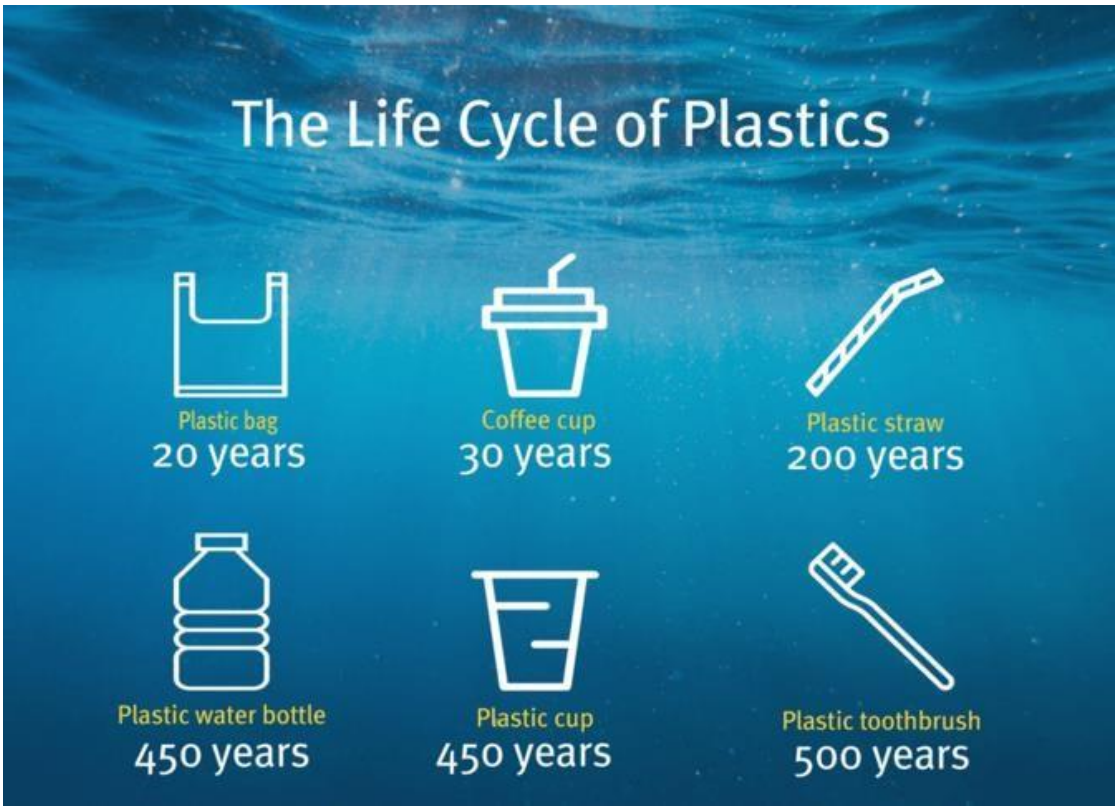

Figure 3. The life cycle of plastics.

The figure illustrates the persistence of different plastic products after disposal, highlighting how long various materials remain in the environment before degrading. Adapted from data provided by WWF (2025).

surroundings, including harmful pesticides, heavy metals, and persistent organic pollutants (Teuten et al., 2009). When ingested by marine life, terrestrial animals, or even humans, these toxins can enter the food chain, leading to severe consequences for both biodiversity and public health (Rochman et al., 2013).

The presence of microplastics is not confined to the oceans. Soil is increasingly being recognized as a major site of microplastic accumulation. It is clear that soils are at significant risk of contamination, since 89% of global plastic waste ends up on land (Morris et al., 2020). The sources of microplastics in soil are diverse, ranging from agricultural films and plastic mulches to improperly disposed waste materials. Once microplastics enter the soil, they can reside there for many years without being removed due to their small size. As a result, the contamination of soil with microplastics has significant implications for agriculture, as these particles can interfere with plant growth, soil structure, and microbial activity.

Research has shown microplastic particles can restrict vegetative growth, inhibit photosynthetic efficiency, and reduce reproductive success in plants (Qi et al., 2018; Ren et al., 2021; Tian et al., 2022), whilst also disrupting the way soil retains water, alters nutrient cycling and affects the balance of soil microorganisms, which in turn impacts plant growth and crop yields (Rillig et al., 2020). The long-term effects of this disruption are still not fully understood, but microplastics in soil could contribute to significant challenges in global food security.

Alarmingly, microplastics are now making their way into compost as the separation of plastic particles from organic waste is not adequate. Composting is a common method used to recycle organic waste and enrich the soil, yet it has become a way for microplastics to be spread out further. Given that compost is often used in agricultural practices to enhance soil health, this becomes a serious concern. The introduction of microplastics into compost could lead to their spread in agricultural fields, increasing the risk of contamination in the food chain. This revelation only amplifies the problem as the more ecosystems affected by microplastics, the more avenues they have to enter the food chain.

It is critical to focus efforts on understanding the presence and behaviour of microplastics in compost. The ability to detect these particles early and accurately can help us gauge the extent of their presence in agricultural systems. This is not only essential for understanding the broader environmental implications but also for mitigating the impact they have on plant growth and soil health. This study aims to develop and evaluate the technique of SSNMR to determine whether it is a reliable method for identifying microplastics in compost and potentially track their degradation over time.

Current methods for detecting microplastics in environmental samples, such as FTIR or Raman spectroscopy, are effective but come with certain limitations. These methods often require extensive sample preparation and can fail to detect small quantities of plastic when mixed with an excess of materials like compost. SSNMR could potentially eliminate these limitations and help assist studying microplastics in compost; it is a non-destructive technique allowing materials to be studied in their natural state, without altering their chemical structure or composition. This makes it particularly suited for analysing compost, as it will enable the tracking of microplastics and their interaction with organic matter over time without introducing any bias or distortion into the data.

Conventional non-biodegradable plastics have a life expectancy of hundreds to thousands of years, whilst biodegradable plastics may be able to decompose in a couple of months with sufficient humidity, oxygen and microorganisms (Moshood et al., 2022). However, even with biodegradable plastics, the degradation process is not fully understood. Whether SSNMR can clearly show polymer presence and potential degradation in a spectra, depends on how the degradation differs between types of plastics, whether the compost and polymer peaks overlap, and how a change in pH affects the results. This could provide valuable insight into how composting conditions influence the degradation of microplastics and open up new possibilities for accelerating the breakdown of plastics in environmental systems.

2.2 The Importance of Compost

Compost is an organic mixture of plant nutrients that uses microorganisms to turn it into a material suitable for agriculture (Christian, n.d.), differing from soil which is simply a natural earth material. Compost is used to enrich soil with the nutrients, as it is made from biodegradable materials from different original sources, it has higher chance of mixing with microplastics.

Microplastics have been present in the environment since the early production of plastics. There are two variations of microplastics that depend on their origin in the environment:

- **Primary Microplastics –** Micro-sized plastic objects manufactured purposefully for specific applications

- **Secondary Microplastics –** Found in the environment as fragmentations of larger plastic products by mechanical, chemical, radiation, or biological degradation.

As the importance of compost in agriculture only expands, ensuring there is no contamination from microplastics that can easily leak into crops is particularly important. Microplastic contamination needs analytical tools that can quickly and accurately confirm the contamination levels of a sample. This project explored SSNMR as a method to detect microplastics in compost. The major benefit is that it can analyse multiple samples mixed together without needing to break them down or isolate individual components. This is particularly useful when dealing with complex materials such as compost.

This exploratory research aims to determine if SSNMR is a suitable technique to identify synthetic polymers dispersed of a natural, organic matrix. Previous techniques have been used to identify and analyse this area, with limited results. SSNMR has been used previously when analysing the organic matter in compost (Pizzanelli et al., 2023) but using this technique to analyse different plastics in compost is unexplored.

2.3 Challenges in Detecting Polymer Degradation

One of the major scientific challenges in using SSNMR to monitor microplastics in compost is the detection of polymer degradation. Nonbiodegradable plastics like PE and PP degrade extremely slowly under natural soil conditions — often taking years or even decades (Alsabri et al., 2022). This limits the feasibility of observing meaningful degradation within a typical research time limit.

Biodegradable plastics, such as PLA and TPS, degrade up to 20 times faster, but even these materials show minor structural changes in shortterm studies. If degradation occurs, it raises another complication; if the polymer breaks down into monomers or smaller fragments, they may no longer appear as distinguishable peaks in the SSNMR spectrum. These chemical shifts might blend with the background compost signals, making them difficult to identify. It is important, therefore, to establish the limitations of SSNMR in this context, as well as its strengths.

Studies using FTIR or thermal analysis have noted similar challenges with identifying the products of polymer breakdown as an overlap of peaks limits the information available and requires careful calibration to solve (Haas, 2023). This issue is especially relevant for this research, as it ties directly into whether SSNMR can be used not just for detection, but also

for monitoring degradation dynamics over time. This investigation will begin to address these unknowns and assess whether changes in pH or microbial activity can produce detectable shifts in the SSNMR signal, giving us a way to track how degradation unfolds.

2.4 Using SSNMR to Study Compost

Previous research has shown that SSNMR can be used to study the organic content of compost, which makes it a promising analytical tool for exploring complex environmental samples (Cardoza et al., 2004).Unlike solution-based NMR, SSNMR does not require the sample to be dissolved, meaning it can analyse solids like compost directly, without breaking apart the natural structure or interfering with the chemical environment.

This is especially relevant for studying microplastics in compost, as it allows us to analyse both the plastic and the organic matter together, in situ. The literature so far has focused mostly on understanding compost composition using SSNMR, but has not extended to tracking synthetic polymers within that matrix. This gap suggests untapped potential for applying the technique to microplastic contamination.

2.5 Why SSNMR Has not Been Used for Microplastics

Despite the potential advantages of SSNMR for studying plastics in soils and compost, it has not yet been widely adopted for this purpose, and its strengths and limitations have not been examined. Most of the existing analytical methods (e.g., FTIR, Raman spectroscopy and pyrolysis-GC/MS) are well-established, but often require sample preparation steps like digestion, extraction, or filtration, which can alter the sample's natural state or even introduce contamination.

By contrast, SSNMR could allow direct analysis of solid compost samples without requiring destructive processing. This means it might provide a clearer picture of microplastic presence and behaviour within compost as it exists in real conditions. Still, this potential remains theoretical as the literature shows almost no application of SSNMR for directly detecting plastic polymers in mixed organic environments (Keeler & Maciel, 2003; Kögel-Knabner, 1997; Lorenz et al., 2006; Preston, 1987; Wang & Nielsen, 2020). This absence highlights a need for experimental work to test the method’s capabilities and limitations. A disadvantage of NMR compared to other techniques is its low sensitivity, a consequence of the Boltzmann populations of atomic nuclei in the superconducting magnetic fields of modern NMR spectrometers.

2.6 NMR theory section

Nuclear Magnetic Resonance (NMR) spectroscopy is a powerful analytical technique that exploits the magnetic properties of certain atomic nuclei to provide detailed information about molecular structure and dynamics. Nuclei such as ^{1}H and ^{13}C possess a nuclear spin, which gives rise to a magnetic moment. When placed in a strong external magnetic field (B_0), these nuclei align either with or against the field, creating discrete energy levels. By applying a radiofrequency (RF) pulse at the resonance frequency specific to each nucleus, transitions between these spin states are induced. The resulting signal, known as the free induction decay (FID), is detected and transformed into a spectrum via Fourier transformation, revealing the chemical environments of the nuclei (Keeler, 2011).

A key feature of NMR is the chemical shift (δ), which reflects the local electronic environment surrounding a nucleus. This shift is measured in parts per million (ppm) relative to a standard reference compound and allows for the identification of functional groups and molecular architecture. However, the utility of NMR extends beyond structural elucidation—it also provides insights into molecular motion through nuclear relaxation processes.

Two primary relaxation mechanisms govern how nuclei return to equilibrium after excitation: longitudinal relaxation (T_1) and transverse relaxation (T_2). T_1, or spin-lattice relaxation, involves the transfer of energy from the excited nucleus to its surrounding lattice and is sensitive to molecular mobility. Short T_1 values typically indicate dynamic, disordered environments (e.g., hydrated compost), while long T_1 values are characteristic of rigid, crystalline materials like polyethylene (Levitt, 2008). T_2, or spin-spin relaxation, describes the loss of phase coherence among spins and directly influences peak width—short T_2 values result in broader, less resolved signals.

In solid-state NMR (SSNMR), line broadening is a significant challenge due to anisotropic spin interactions that are not averaged out as they are in solution-state NMR. These include chemical shift anisotropy (CSA) and dipole-dipole couplings, which depend on the orientation of the molecule relative to the magnetic field. To overcome this, Magic-Angle Spinning (MAS) is employed. By spinning the sample rapidly at an angle of 54.74° relative to B_0—the so-called magic angle—these anisotropic interactions are averaged, resulting in narrower, more interpretable peaks (Andrew et al., 1958).

Further enhancement of spectral resolution and sensitivity is achieved through high-power proton decoupling, which removes heteronuclear dipolar interactions during acquisition, and Hartmann-Hahn crosspolarisation (CP). CP transfers magnetization from abundant ^{1}H nuclei to less sensitive nuclei like ^{13}C by matching their RF fields, significantly boosting signal intensity, and reducing acquisition times (Hartmann & Hahn, 1962). This technique is particularly effective for rigid systems with strong dipolar couplings, such as polymers and bioplastics, making it ideal for studying materials in composting environments.

Together, these principles and techniques make SSNMR a uniquely powerful tool for probing the molecular structure and degradation behaviour of polymers in complex matrices. Its ability to distinguish between rigid and mobile domains, resolve overlapping signals, and track chemical changes over time underpins its growing role in environmental and materials research.

2.7 Differentiating Plastics from Compost Using T_1 Relaxation

One key reason SSNMR could work for detecting microplastics in compost is due to differences in nuclear relaxation behaviour between organic material and synthetic polymers. Specifically, T_1 relaxation times — which describe how quickly nuclei return to equilibrium after excitation — vary significantly between compost and common plastics (Haber-Pohlmeier et al., 2010).

This difference allows for potential signal isolation. In theory, by adjusting acquisition parameters based on these relaxation times, it is possible to selectively detect polymers even in small concentrations. However, practical demonstration of this principle, particularly in real-world compost scenarios, is lacking. This study aims to explore this theoretical separation and determine whether it is dependable and sensitive enough to work under controlled experimental conditions.

3. Materials and Methods

3.1 pH changing chemicals

Any chemical used for changing pH of the compost or inducing a chemical degradation to a polymer was from the Biomedical and Life Sciences lab at Lancaster University.

3.2 Source of plastics

All plastics were received as kind gifts from two manufacturers, in pellet or in a bag form of some kind, from a non-woven to a more traditional plastic bag. Table 1 shows the plastics and bioplastics used in this research and their suppliers. Every polymer was provided by a manufacturer from their product portfolio. PP and PE were chosen for the study as adequate samples were provided throughout the research. Bioplastics were represented by a range of biodegradable plastic bags provided by a single manufacturer. This gave the research an authenticity, being able to examine real world products, which is important as a major theme throughout this project is the ties to the real world and the attempts to be as natural as possible.

Table 1. Polymers chosen for analysis. Biodegradable plastics shown with a (BD).

Polymer	CAS	Biodegradable?	Obtained from	Form obtained
PP	9003-07-0	No	Alpla Oil Refineries LTD	Sheet and Pellet
LDPE	9002-88-4	No		
HDPE	9002-88-4	No		
PLA	26100-51-6	Yes	Bioapply	Company manufactured bag
Corn Starch Based (TPS)	9005-25-8	Yes		
Potato Starch Based (TPS)	9005-25-8	Yes		
PLA based	26100-51-6	Yes		

Each non-biodegradable polymer acquired was obtained in its pure form with no additives noted to be present. Whilst the biodegradable polymers came with additives mixed into the product, apart from the pure PLA bag. The two thermoplastic starch (TPS) products had been combined with PBAT and PBST to make the plastic. To distinguish between the two products, the terms 'Potato Starch' and 'Corn Starch' are used. The PLA-based bag is a mixture of PLA, PBAT/PBST and $CaCO_3$, with only 10% being PLA.

Products labelled as based were mixed with PBAT and PBST, which have the CAS numbers 60961-73-1 and 25777-14-4, respectively.

3.3 Preparation of plastics

A minimal amount of pre-treatment of the plastics was necessary before combining with compost for analysis, to ensure that the polymers could be dispersed evenly throughout the compost. This was important (i) to increase the surface area to enhance degradation and (ii) for reproducibility purposes when taking multiple samples from the same bulk compost-polymer mixtures for SSNMR analysis.

Some polymers were obtained in a pellet form (1-5 mm diameter) that required milling. Two milling approaches were tested. One method used liquid nitrogen to flash-freeze the pellets, followed by grinding with a pestle and mortar. This method was found to be inefficient, owing to the limited period the pellets remained frozen. An alternative and more efficient method using a cryomill (where and what model?) was therefore used to convert the pellets into a powdered microplastic form (>1µm) (Patil et al., 2020). To the cryomill was added 0.5mg of each plastic, which was cooled for 7.5 minutes, followed by 5x 3 minute milling sessions (at 250Hz) with a 1.5 minute rest period in between. This process resulted in consistent milling which broke up every pellet into fine microplastics ready for use.

For the biodegradable plastics that were already in a bag form, to make them into a sample size small enough to fit in the rotor, a 2.5mm hole punch was used to take small samples of the bag and use them to create the compost mixtures.

3.4 Preparation of compost and plastic samples

The compost was sampled from the same original source, a standard commercially sourced compost that was deemed to have the right balance of organic matter and microorganisms to help in the degradation process. Before being weighed and added to a sample tube, compost was ground up using a pestle and mortar to break up any larger pieces and to help minimise the amount of sticks and stones found in the compost, which would not fit in the SSNMR rotor and would limit space for the intended products.

Plastic samples were then mixed thoroughly into the compost sample to ensure as even distribution as possible. Easier with the ground polymers as their powder like physical appearance spread out much better in the sample. Samples were made up of 2.5g of compost and 100mg of plastic,

except for samples comparing the ratio of compost to polymer when evaluating the usefulness of SSNMR

The pH was monitored with indicator paper throughout the experiment to ensure the pH stayed constant throughout the experiment. The control compost sample was at pH 7. In some experiments, the pH of compost was altered to determine whether a change in pH affected degradation time in polymers and bioplastics. This was done by adding a solution of NaOH, HCl or Tris Buffer depending on the desired pH. To every 2 g of compost, 1mL of pH modifying solution was added before being stirred together first manually and then centrifuged on a bench-top centrifuge to remove excess liquid. The modified compost was then measured by pH paper to ensure the modifier had succeeded in raising or lowering the compost. Paper was only used after the compost and modifier had had time to equilibrate to ensure the paper was not simply recording a change in pH due to the modifier.

3.5 Sample aging

Samples were stored in a humidifier at 19 °C and 99% humidity. Humidity and temperature were tracked constantly using a hygrometer to ensure consistency in the storage. If a sample was deemed to be too moist after centrifugation, it was incubated in a glass oven at 65°C for 2 hours to remove any excess solution in the sample. A compost sample being too moist could potentially negatively affect the signal-to-noise ratio of the SSNMR spectrum.

3.6 Analytical techniques used

All analytical equipment used were based in the Lancaster University Chemistry department.

3.6.1 FTIR Analysis

FTIR was used to act as a benchmark technique for analysis of the polymers obtained, to ensure they followed previous spectra found throughout the literature. Measurements were taken using FTIR (Insert specs here) by performing 8 scans. In transmittance mode, from 750 cm^{1} to 3250 cm^{-1} with a scanning resolution of 4 cm^{-1}.

3.6.2 X-ray fluorescence (XRF)

In order to ensure there were no substantial amount of minerals present in the compost that could affect the spectra results, XRF analysis was performed on a humid and dry sample of the control compost in the

absence of polymer. This control was analysed by XRF (EDX-8000) for 5 minutes in a Mylar sample cup. With each mineral present in the sample along with the organic matter present in the compost all shown in Table 3 and 4.

3.6.3 SSNMR

3.6.3.1 Experimental set-up and criteria

All ^{13}C SSNMR analysis was carried out at Lancaster University using a Bruker AVANCE III HD 700 WB NMR system equipped with UltraShield Plus wide-bore (89mm) 16.4T magnet. All SSNMR experiments employed magic-angle spinning (MAS) at a rate of 6500 Hz in a 3.2mm rotor. For the majority of the experiments, 20,480 scans were taken for each spectra, with a recycle delay of 2 s, as an acceptable compromise between instrument availability, sample throughput, and signal-to-noise of the spectrum.

Compost samples were transferred to a 3.2 mm diameter zirconia MAS rotor fitted with a Kel-F cap. The internal volume of the rotor was approximately 30 mL, and so it was important to pack the sample as tightly as possible to maximise the signal-to-noise of the SSNMR experiment. As the bioplastics from bags were collected via 2.5mm holepunches, the 3.2mm rotor with an inner diameter of 2.6mm was deemed to be the rotor that fit the criteria the best. Due to the importance of keeping the conditions as natural as possible, room temperature was used as a control throughout the experiments. It was ensured that the 3.2mm rotor used would be between 66-75% full to maximise the amount of product being analysed whilst leaving space for the cap and allowing the spinning to commence smoothly. Products, ground as described above, were packed tightly into the rotor with gentle compression.

3.6.3.2 Specific experimental parameters

All SSNMR experiments employed ^{13}C detection with proton decoupling during signal acquisition. Basic one-dimensional (1D) experiments employed a 3 ms ^{1}H excitation pulse followed by 2 ms Hartmann-Hahn CP from ^{1}H to ^{13}C at a ^{1}H spin-lock frequency of 63 kHz. Proton decoupling at 83 kHz using the SPINAL-64 sequence was applied during signal acquisition. Spin-lattice relation rates of ^{1}H and ^{13}C were measured using ^{13}C-detected inversion recovery sequences. For ^{13}C T_1 measurements, the pulse sequence p/2 (^{1}H)-CP-p/2 (^{13}C)-t-p/2

(^{13}C)acquire was used. The ^{13}C p/2 pulse length was 4 ms. For 1H T1 measurements, the pulse sequence p (^{1}H)-t - p/2 (^{1}H) – CP was used.

Spectra were processed using TopSpin 3.2pl6 and 3.5pl7, with licenses for NUS and Protein Dynamics Center.

3.7 Solution-State NMR

Solution-state ^{1}H NMR was carried out at Lancaster University using a Bruker Avance Neo 400 equipped with a 5mm ^{1}H-X broadband observe (BBFO, ^{109}Ag-^{19}F) RT iProbe and a 60-position SampleCase Plus autosampler. The instrument was controlled with TopSpin 4.5.0 on Windows 11. Samples that were analysed using Solution-State NMR were bioplastics that had been left to break down in NaOH for a couple of hours or days depending on the sample.

4. Results

4.1 Overview

With the focus being on SSNMR as a technique, a variety of polymers and biopolymers were used for the analysis to ensure the method was successful with a variety of products. This is partly to help with the validity and reliability of the experiments, as being able to repeat results with different polymers is a key component when evaluating the technique. Microplastics are all different chemically, so being able to determine which types of microplastics fare better in the analysis is useful information that could easily be expanded. With the polymers, there was no expectation in being able to see any degradation take place due to the previously mentioned understanding of the average degradation time of plastics. However, the aim for plastics was seeing whether they could be detected rather than being able to tell if they had degraded, which was confirmed.

Focusing on bioplastics, being the expected product to degrade in a much shorter period in time, we learnt how little product was required for it to be detected and how the inconsistencies in taking samples can really affect the spectra.

4.2 FTIR analysis

FTIR was used as a rapid and convenient technique to characterise the non-biodegradable polymers before addition to the compost, to confirm their chemical composition.

4.2.1 Polypropylene (PP)

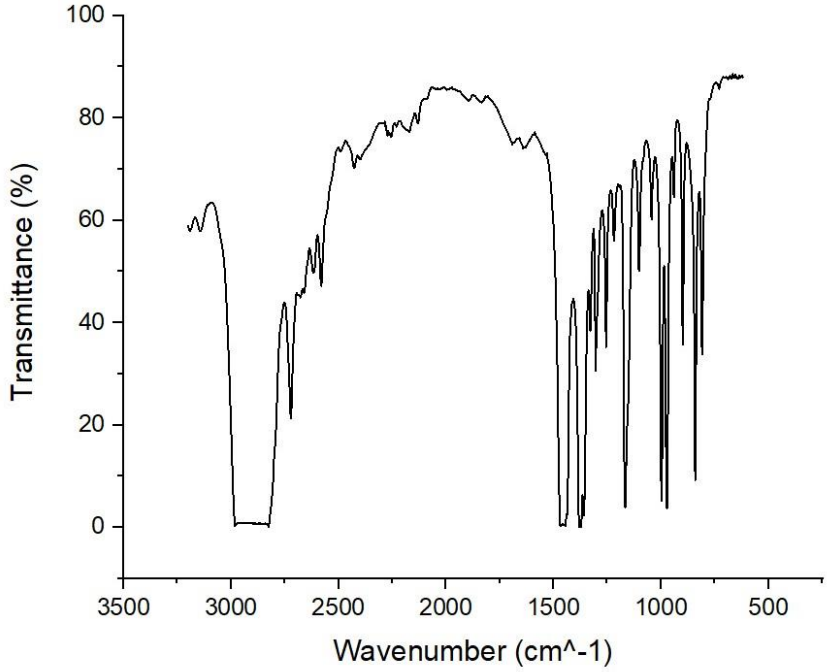

Figure 4. FTIR spectra of polypropylene by measuring Transmittance (%) against Wavenumber (cm^{-1}).

Figure 4 shows the spectrum of polypropylene (CAS 9003-07-0). The spectrum features the expected strong -CH stretching vibrations around 2950-2840cm^{-1} for asymmetric and symmetric CH_3 and CH_2 bonds, with bending vibrations around 1455 and 1375cm^{-1} for CH_2 and CH_3 bonds, respectively. The fingerprint region (below 1250cm^{-1}) has bands relating to C-C stretching and bending, as well as peaks that are typical for crystalline isotactic PP and arise from skeletal vibrations of the polymer's backbone.

4.2.2 Polyethylene (PE)

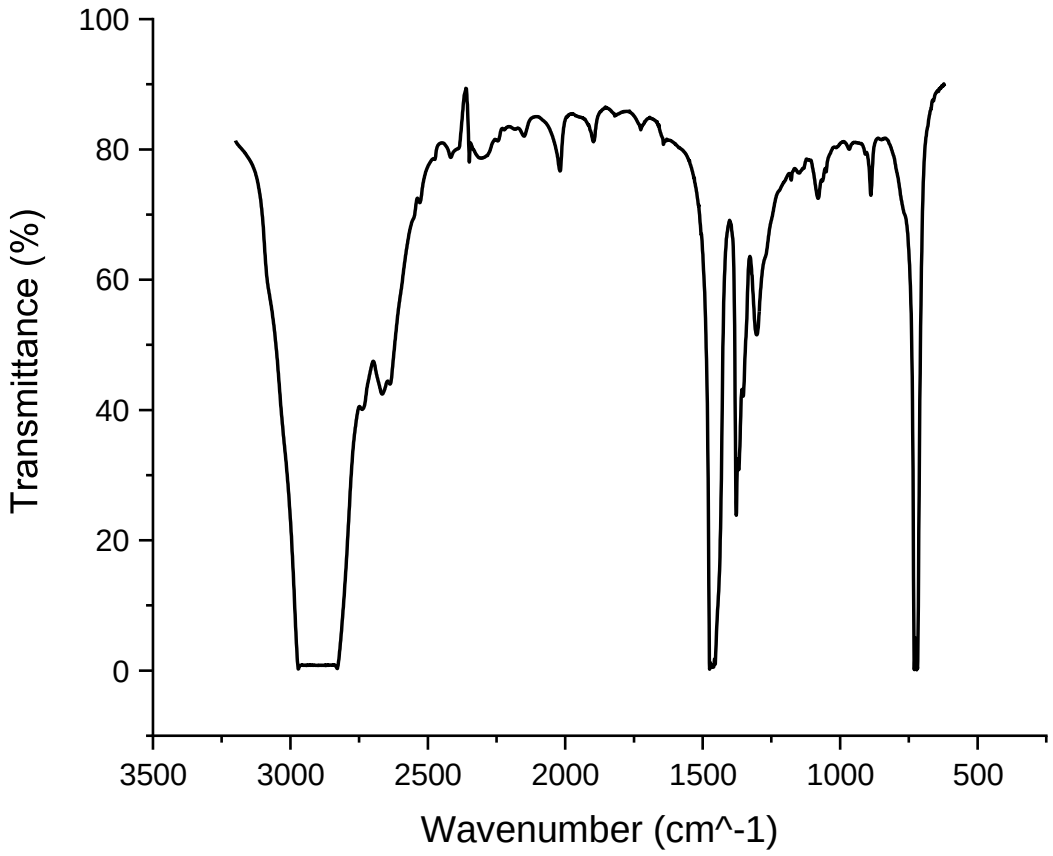

Figure 5. FTIR spectra of Polyethylene by measuring Transmittance (%) against Wavenumber (cm^{-1}).

Figure 5 shows the spectrum of polyethylene (CAS 9002-88-4). The spectrum features strong peaks at ~2915cm^{-1} and ~2848cm^{-1}, corresponding to the asymmetric and symmetric stretching of CH_2 bonds. The bands at ~1472cm^{-1} and ~1463cm^{-1} arise from CH_2 scissoring and bending vibrations, whilst the weak band at ~1377cm^{-1} is potentially from a CH_3 bending bond due to a terminal group or potential branching in the polymer chain. The fingerprint region indicates two rocking vibrations at ~730cm^{-1} and ~718cm^{-1}, representing the presence of both crystalline and amorphous phases of PE.

4.3 X-Ray Fluorescence

The elemental composition of the compost samples was characterised using X-ray fluorescence (XRF), providing quantitative insight into both the inorganic mineral fraction and the proportion of organic matter.

Across both humid and dry samples, silicon, calcium, and aluminium were identified as the dominant mineral components, reflecting the presence of soil-derived silicates and plant-based residues within the compost matrix. Iron (Fe) and manganese (Mn) were also detected at measurable levels, which is particularly relevant for the subsequent SSNMR experiments. These metals possess unpaired electrons and therefore act as paramagnetic centres, enhancing nuclear relaxation processes and potentially shortening T_1 and T_2 relaxation times. Such effects can contribute to line broadening and reduced spectral resolution in solid-state NMR. All elemental concentrations were calculated using the Fundamental Parameters (FP) method (Quan-FP), which is well-suited for heterogeneous matrices such as compost where direct calibration standards are not easily applied.

Table 2. Compost content under humid conditions analysed via X-Ray Fluorescence (XRF)

Analyte	**Result**	**[3-sigma]**	**Proc.-Calc. Line**		**Int.(cps/µA)**
Si	4.464 %	[0.060]	Quan-FP	SiKa	1.0801
Ca	1.529 %	[0.005]	Quan-FP	CaKa	15.8371
Al	1.406 %	[0.122]	Quan-FP	AlKa	0.0660
K	0.857 %	[0.005]	Quan-FP	K Ka	5.5544
Fe	0.611 %	[0.002]	Quan-FP	FeKa	186.4535
S	0.257 %	[0.004]	Quan-FP	S Ka	0.5863
P	0.213 %	[0.014]	Quan-FP	P Ka	0.1514
Ti	0.092 %	[0.001]	Quan-FP	TiKa	6.3787
Mn	0.024 %	[0.001]	Quan-FP	MnKa	5.2997
Zn	0.011 %	[0.000]	Quan-FP	ZnKa	7.2699
Pb	0.007 %	[0.001]	Quan-FP	PbLb1	2.3277
Sr	0.006 %	[0.000]	Quan-FP	SrKa	5.7732
Cu	0.004 %	[0.000]	Quan-FP	CuKa	2.4066
V	0.004 %	[0.001]	Quan-FP	V Ka	0.4231
Rb	0.002 %	[0.000]	Quan-FP	RbKa	2.2621
Br	0.002 %	[0.000]	Quan-FP	BrKa	1.6650

Organic Matter	90.510 %	[---------]	Balance	------	---------- ---

Table 3. Compost content under dry conditions analysed via XRF.

Analyte	**Result**	**[3-sigma]**	**Proc.-Calc. Line**		**Int.(cps/µA)**
Si	13.879 %	[0.128]	Quan-FP	SiKa	2.7565
Ca	4.976 %	[0.015]	Quan-FP	CaKa	28.0436
Al	3.872 %	[0.133]	Quan-FP	AlKa	0.1679
K	2.681 %	[0.012]	Quan-FP	K Ka	10.2594
Fe	1.839 %	[0.005]	Quan-FP	FeKa	264.6966
P	0.825 %	[0.014]	Quan-FP	P Ka	0.3786
S	0.793 %	[0.010]	Quan-FP	S Ka	1.1469
Ti	0.261 %	[0.004]	Quan-FP	TiKa	8.9034
Mn	0.107 %	[0.001]	Quan-FP	MnKa	11.1550
Zn	0.032 %	[0.001]	Quan-FP	ZnKa	10.2519
Pb	0.017 %	[0.001]	Quan-FP	PbLb1	3.3494
Sr	0.014 %	[0.000]	Quan-FP	SrKa	9.0295
Rb	0.014 %	[0.000]	Quan-FP	RbKa	8.3818
Cu	0.012 %	[0.001]	Quan-FP	CuKa	3.1065
V	0.010 %	[0.002]	Quan-FP	V Ka	0.5292
Cr	0.005 %	[0.001]	Quan-FP	CrKa	0.4250
Br	0.004 %	[0.000]	Quan-FP	BrKa	2.3053
Y	0.001 %	[0.000]	Quan-FP	Y Ka	0.9234
Organic Matter	70.656 %	[---------]	Balance	------	---------- ---

The XRF results show clear compositional differences between the humid and dry compost samples. The humid compost appears to contain a much higher proportion of organic matter (≈ 90.5%), but this value is inflated by the substantial moisture content, which contributes to the total mass and therefore reduces the apparent mineral percentage. In contrast, the dry compost contains far less water and consequently reveals a higher true mineral load (≈ 29%), including elevated concentrations of Fe, Mn, Ti, and other trace metals. This increased

abundance of paramagnetic species in the dry sample is expected to exert a stronger influence on SSNMR behaviour, producing shorter relaxation times and broader, less resolved spectral lines. Meanwhile, the humid compost, although lower in paramagnetic metals, introduces its own form of spectral broadening through increased molecular mobility and structural disorder associated with moisture. Together, these XRF-derived differences provide essential context for interpreting the variations in relaxation behaviour and spectral quality observed in the SSNMR experiments.

4.4 SSNMR analysis

4.4.1 Control sample of Compost

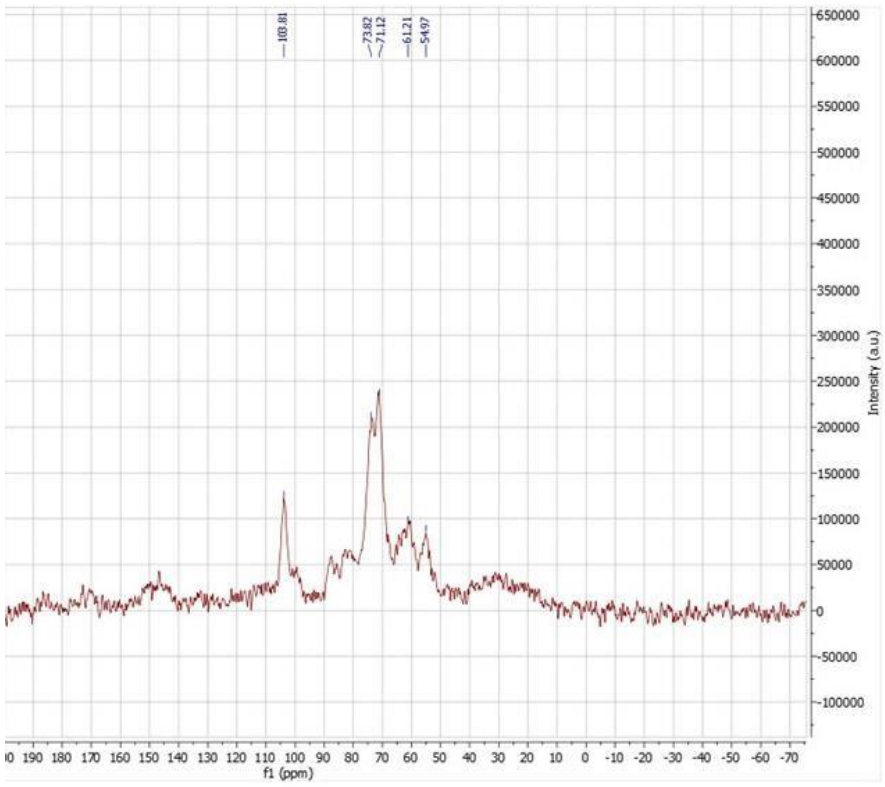

Figure 6. Solid-State ^{13}C NMR Spectra of a control sample of compost by measuring Intensity (a.u.) against Chemical Shift (ppm) seen as f1. *Features major peaks at 103.81 ppm, 73.82 ppm, 71.12 ppm, 61.21ppm and 54.97 ppm.*

The compost sample in the absence of polymer was analysed by ^{13}C CP-MAS SSNMR (Figure 6). The chemical shift dispersion of the most dominant peaks reflects the rich array of carbon environments present in the organic matter. Peaks between 60-90 ppm are typically associated with plant-derived polysaccharide such as cellulose and hemicellulose. Given that the peaks cover such a broad range of ^{13}C chemical shifts, it is

possible that the peaks from compost will overlap with some or all of the resonances from the polymer in the mixed samples (see below).

4.4.2 Pure Polymers

The ^{13}C CP-MAS SSNMR spectrum of pure PE is shown in Figure 7.

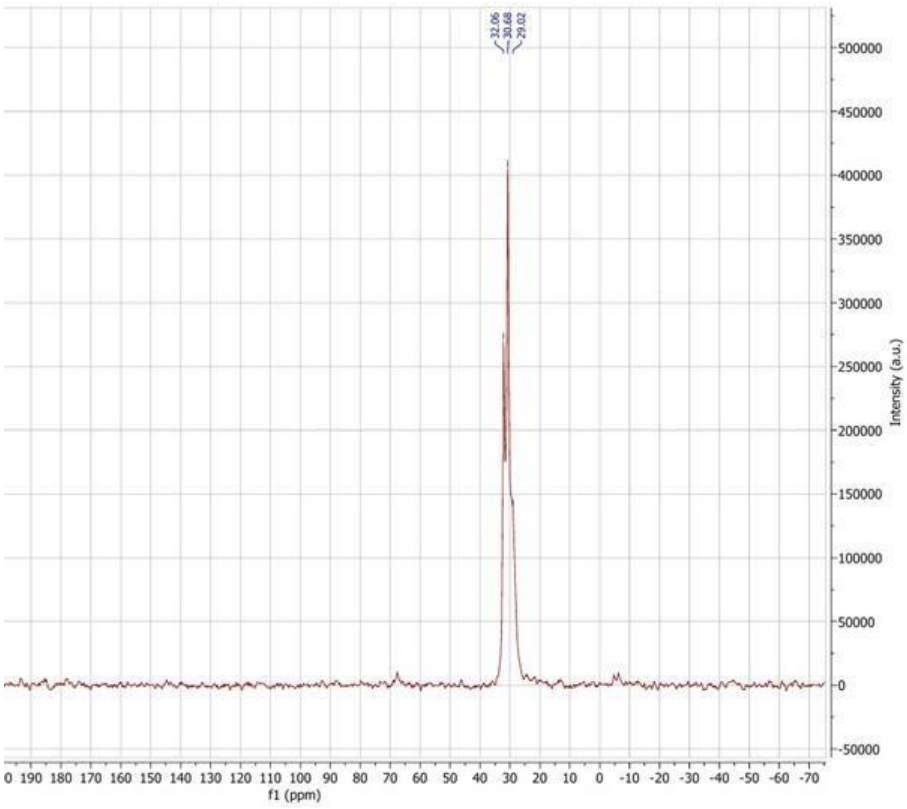

Figure 7. Solid-State ^{13}C NMR Spectra of pure PE by measuring Intensity (a.u.) against Chemical Shift (ppm) seen as f1.

The peak at 29.02 ppm corresponds to the highly ordered crystalline CH_2 groups in the PE backbone. This peak represents the most ordered portion of the PE structure and is indicative of a high degree of crystallinity in PE. The peak at 30.68 ppm corresponds to intermediate crystallinity in CH_2 groups, indicating semi-crystalline or amorphous crystalline mixed regions of the polymer. The peak at 32.06 ppm corresponds to CH_2 groups in regions of PE that are less ordered, with these carbons environments still having some degree of crystallinity whilst being more disordered compared to other regions of the polymer.

The ^{13}C CP-MAS SSNMR spectrum of pure PP is shown in Figure 8.

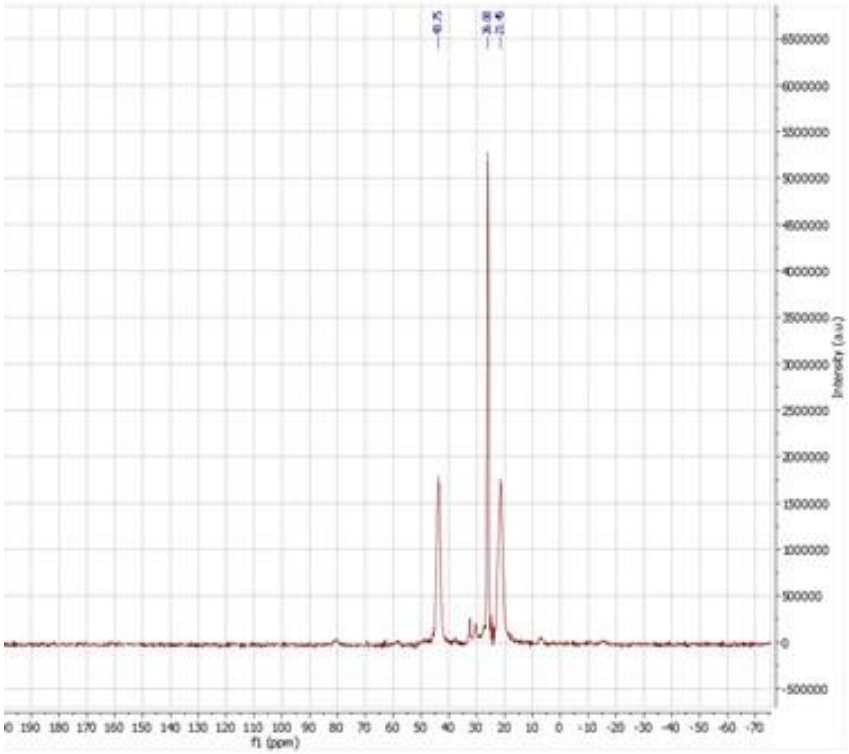

Figure 8. Solid-State 13C NMR Spectra of PP by measuring Intensity (a.u.) against Chemical Shift (ppm) seen as f1.

The peak at 21.45 ppm corresponds to the CH_3 groups in polypropylene (PP). Its position and noticeable broadening suggest that the sample is semi-crystalline, as highly ordered isotactic PP typically exhibits a sharper CH_3 resonance at approximately 20.0 ppm due to its uniform crystalline packing (Bunn & Alcock, 1945; Cheng & Wunderlich, 1986). The peak at 26.00 ppm arises from disordered or amorphous CH_2 environments, which are characteristic of regions with greater chain mobility and structural irregularity; amorphous PP consistently shows broader, upfield-shifted CH_2 signals relative to its crystalline counterpart (Schmidt-Rohr & Spiess, 1994). The resonance at 43.75 ppm is assigned to the CH groups in the polymer backbone, a signal typically associated with the more ordered crystalline lamellae of isotactic PP. Together, the distribution and breadth of these peaks indicate a mixture of crystalline

and amorphous domains, consistent with a semi-crystalline PP morphology.

The ^{13}C CP-MAS SSNMR spectrum of pure PLA is shown in Figure 9. The peak at 16.64 ppm represents the CH_3 group branching off from the backbone and bonded to the chiral centre.

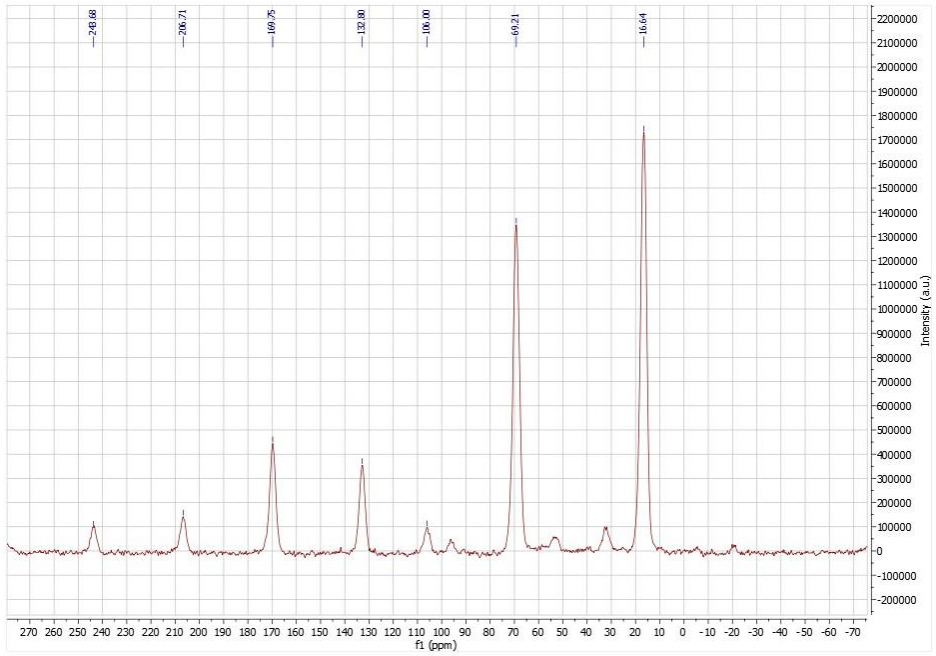

Figure 9. Solid-State 13C NMR Spectra of pure PLA polymer by measuring Intensity (a.u.) against Chemical Shift (ppm) seen as f1.

This peak is consistent with semi-crystalline PLA. The peak at 69.21 ppm corresponds to the CH at the chiral centre which is bonded to the ester and the branched CH_3 group, its intensity and sharpness is consistent with a semi-crystalline structure. The peaks at 106.00 ppm, 132.80 ppm, 206.71 ppm and 243.68 ppm are not expected in a PLA spectra and are therefore most likely from a thermal breakdown of the product causing trace degradation products or potentially the use of a stabiliser. These peaks could also be the result on containment from the synthesis or packaging of this product. The peak at 169.75 ppm corresponds to the carbon in the ester present in PLA and confirms the structure of the PLA polymer is intact and possess repeating ester units.

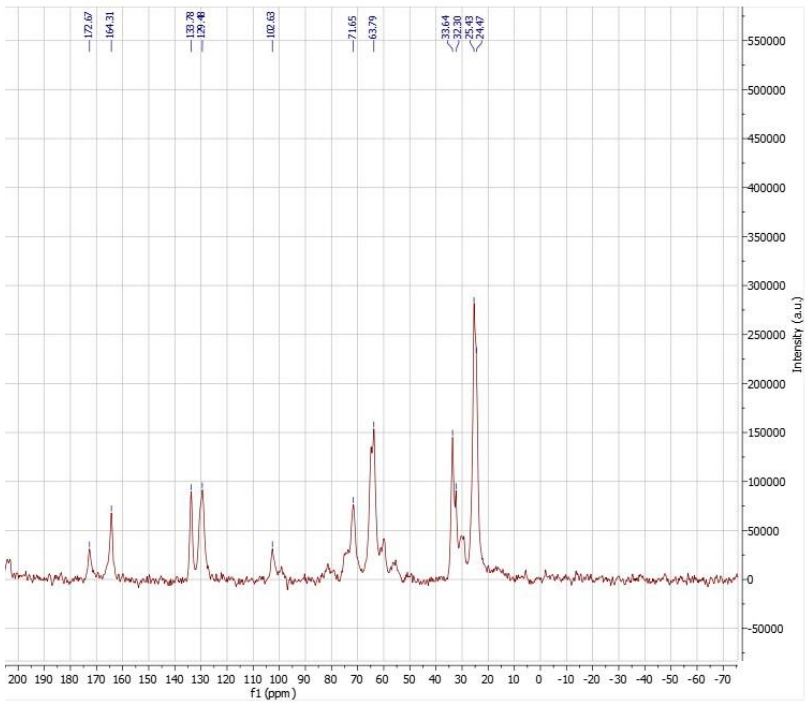

Figure 10. Solid-State ^{13}C NMR Spectra of Potato Starch (TPS) + PBAT/PBST polymer by measuring Intensity (a.u.) against Chemical Shift (ppm) seen as f1.

The peaks at 24.47ppm and 25.43ppm likely represent the central methylene carbons in the PBAT/PBST structure as these are more shielded CH_2 groups, being further from the carbonyls and aromatics present in the polymers. The peaks at 32.20ppm and 33.5ppm correspond to methylene carbons α to teh carbonyl functional groups in PBAT/PBST. The peaks at 63.79 ppm, 71.65 ppm and 102.63 ppm all relate to the cyclic structure present in starch. With each peak representing the primary alcohol carbon, secondary alcohol carbon, and anomeric carbon, respectively. The presence of all three peaks confirms starch is present in this blend. Peaks 129.48 ppm and 133.78 ppm both confirm the presence of CH aromatic carbons from the terephthalate ring in PBAT. The peak at 164.31 ppm is either from an oxidised carbonyl or an electron-deficient ester, as the chemical shift is slightly lower than typical esters. This shift could be due to a chemical modification of starch.

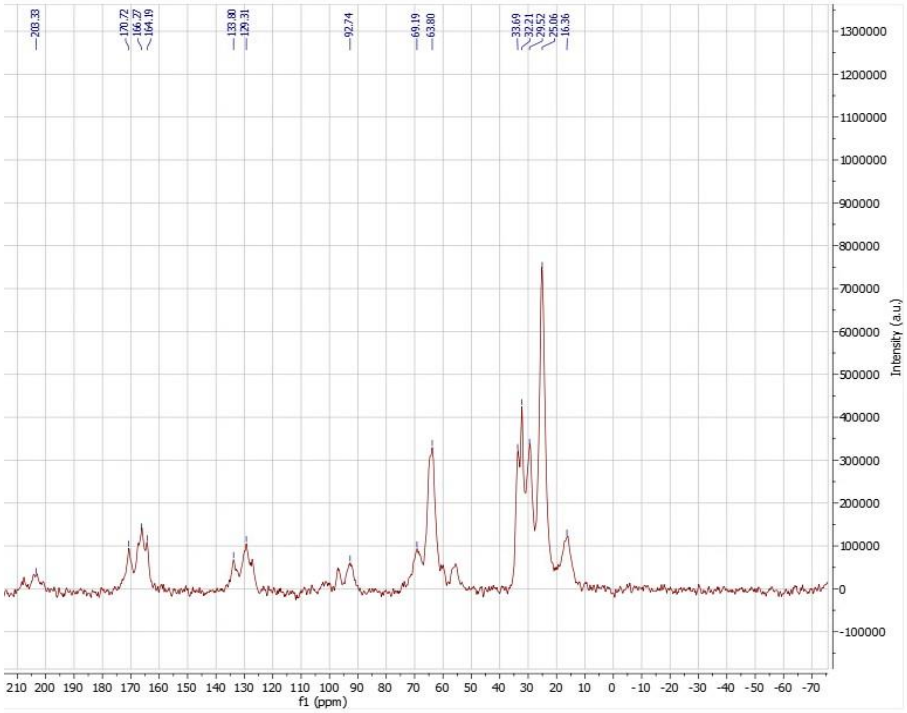

Figure 11. Solid-State ^{13}C NMR Spectra of* Corn Starch (TPS) + PBAT/PBST polymer *by measuring Intensity (a.u.) against Chemical Shift (ppm) seen as f1.

The prominent signals between 20–35 ppm correspond to various aliphatic CH_2 groups. Specifically, the 25.06ppm equates to the most internal methylene carbon, furthest from the carbonyl and aromatic ring. 29.52ppm is a butylene CH_2 closer to a carbonyl group. With 32.21ppm being another carbonyl adjacent CH_2 and 33.69ppm being the CH_2 directly α to the carbonyl functional group.

Further peaks at 63.79 ppm, 71.65 ppm, and 102.63 ppm are characteristic of the cyclic structure of starch. These signals correspond to the primary alcohol carbon (C6), secondary alcohol carbons (C2–C5), and the anomeric carbon (C1), respectively. The presence of all three confirms the intact polysaccharide structure of starch within the blend. Peaks at 129.48 ppm and 133.78 ppm are indicative of CH aromatic carbons from the terephthalate rings in PBAT, confirming the presence of aromatic polyester segments. Finally, the peak at 164.31 ppm arises from a carbonyl carbon in an ester group.

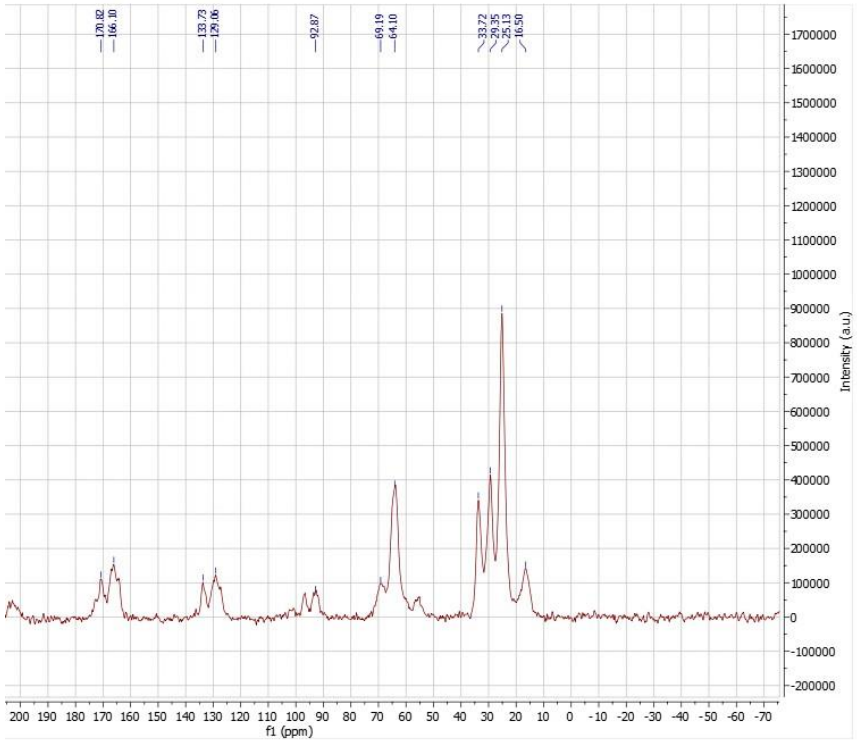

Figure 12. Solid-State ^{13}C NMR Spectra of* PLA + PBAT/PBST + $CaCO_3$ polymer *by measuring Intensity (a.u.) against Chemical Shift (ppm) seen as f1.

Peaks between 16.50ppm and 33.72ppm match up with peaks found in figures 10 and 11, with the CH_3 bond in PLA being considerable smaller compared to the pure PLA sample due to the ratio between the components of the product. Whereas, the PBAT/PBST peaks are strong as expected. The small peak at 92.87ppm is spinning sideband from the aromatic and carbonyl groups.

A distinct resonance near 69–72 ppm confirms the presence of PLA, corresponding to the CH carbon adjacent to the ester oxygen in its backbone. Aromatic carbons from the terephthalate ring in PBAT are evident at 129–134 ppm, while the peak around 164 ppm is attributed to a carbonyl carbon in an ester group.

4.4.3 Polymer and Compost samples

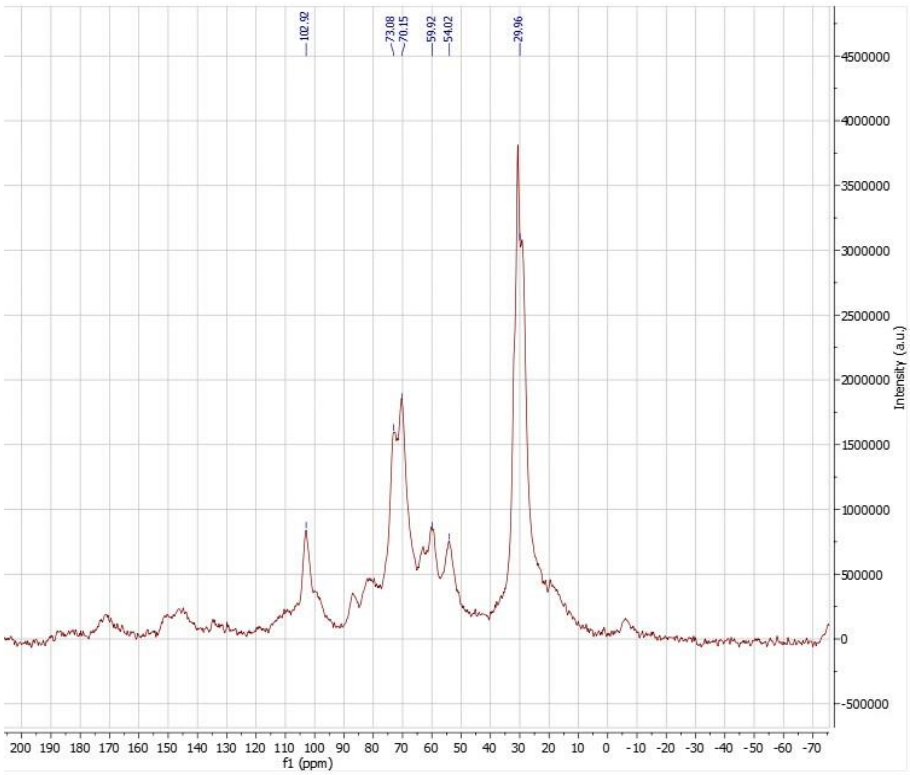

Figure 12. Solid-State 13C NMR Spectra of PE and compost sample by measuring Intensity (a.u.) against Chemical Shift (ppm) seen as f1. *Contains six major peaks, five from the compost at: 102.92 ppm, 73.08 ppm, 70.15 ppm, 59.95 ppm, 54.02 ppm and one from PE at 29.96 ppm.*

Figure 12 shows the spectrum of compost containing PE (20:80).The compost peaks at 102.92 ppm, 73.08 ppm, 70.15 ppm, 59.92 ppm and 54.02 ppm all match up with a peak seen in Figure 6, whilst the PE is only represented with one major peak, being 29.96 ppm. With this peak demonstrating a more uniformed semi-crystallinity throughout the PE sample once being mixed in with compost.

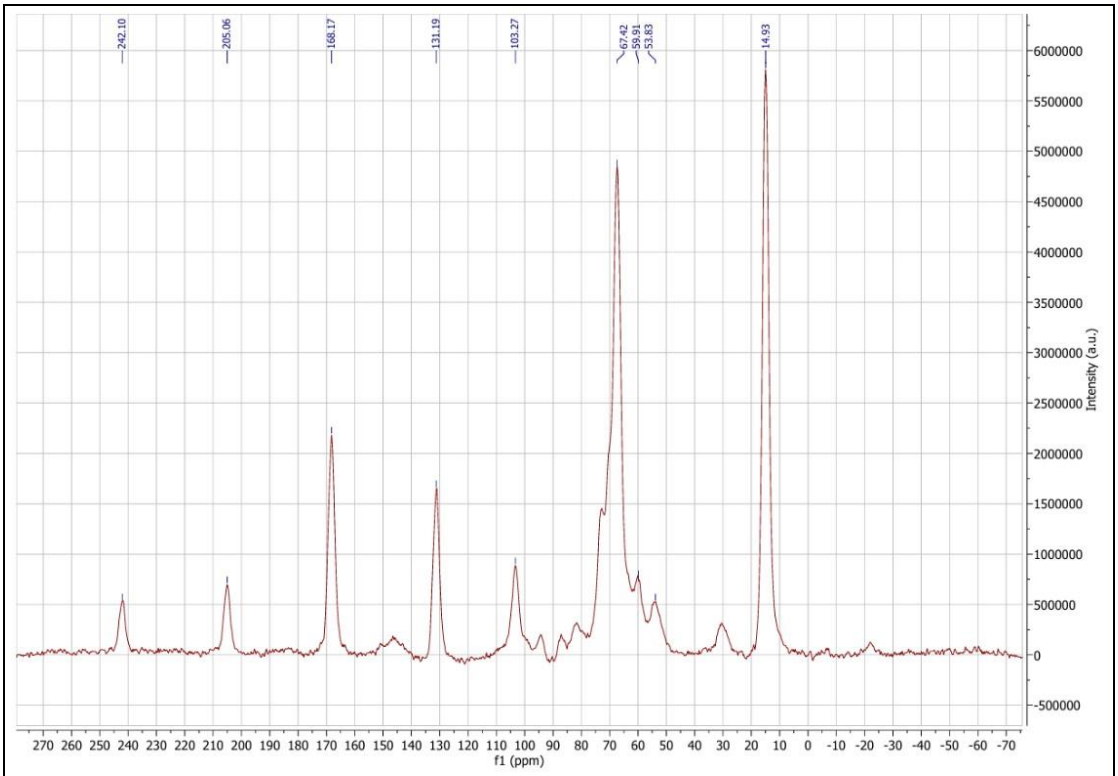

Figure 13. Solid-State ^{13}C NMR Spectra of PLA* polymer *and compost sample by measuring Intensity (a.u.) against Chemical Shift (ppm) seen as f1. *Contains nine major peaks, five from PLA and the other four are contested between the two and just this spectra are not enough to confidently state which peaks are from what.*

Using figure 9 to confirm the peaks that represent the PLA polymer, 242.10 ppm, 205.06 ppm, 168.17 ppm, 131.19 ppm and 14.93 ppm all come from the PLA, whilst peaks at 103.27 ppm, 59.91 ppm and 53.83 ppm are likely to be from compost, we cannot state that for certain PLA has had an effect on them in some capacity. The peak at 67.42 ppm is a combination of both the polymer and the compost as they perfectly overlap at 67.42 ppm due to them both equating to a CH bond.

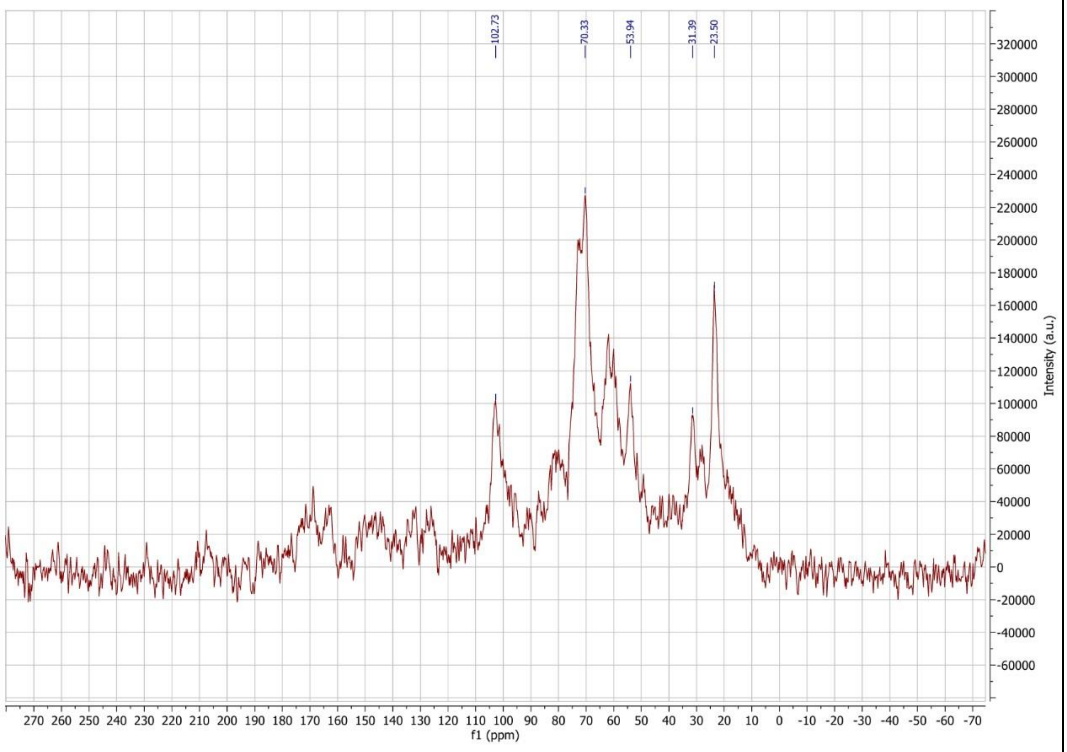

Figure 14. Solid-State ^{13}C NMR Spectra of* Potato Starch (TPS) + PBAT/PBST polymer and compost *by measuring Intensity (a.u.) against Chemical Shift (ppm) seen as f1.

The dominant signals between 20 and 35 ppm remain consistent with aliphatic CH_2 groups from PBAT and PBST and match the peaks from figure 10, with these peaks being slightly broader, due to increased molecular disorder and reduced crystallinity introduced by compost integration.

The starch component is still identifiable through peaks around 72–75 ppm, corresponding to secondary and primary alcohol carbons (C2–C6), although the anomeric carbon near 102 ppm appears less resolved or absent—suggesting partial hydrolysis or reduced signal transfer efficiency. Compost-derived organic matter contributes additional complexity, with overlapping signals and baseline noise that obscure weaker resonances. Peaks at 121–122 ppm remain visible and are attributed to aromatic CH carbons from the terephthalate ring in PBAT, confirming that the polyester structure is retained.

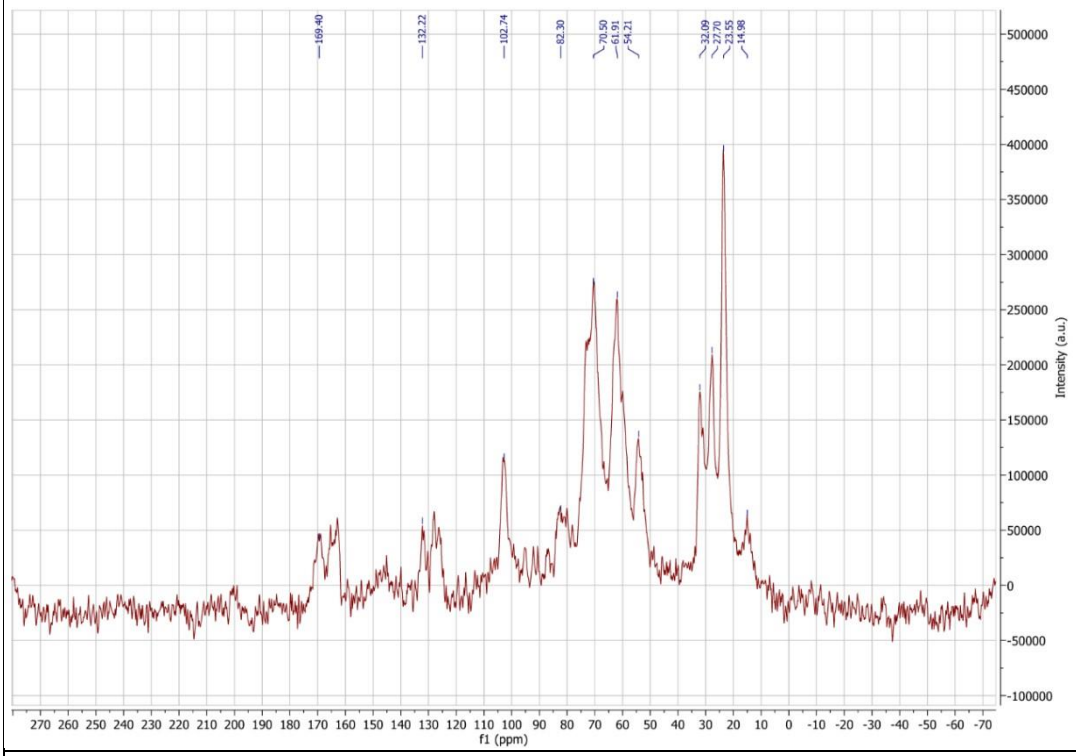

Figure 15. Solid-State ^{13}C NMR Spectra of* Corn Starch (TPS) + PBAT/PBST polymer and compost *by measuring Intensity (a.u.) against Chemical Shift (ppm) seen as f1.

Using figure 11 as a reference point to ascertain what peaks relate to the corn starch-based polymer. The strong signals between 23.55ppm and 32.09ppm are all expected due to the presence of PBAT/PBST and have the same assignment as the peaks in figure 8. The peak at 14.98ppm is likely an alkyl CH_3 / CH_2 from microbial biomass commonly found in compost.

Distinct peaks at approximately 63.8ppm, 71.6ppm, and 102.6ppm confirm the presence of corn starch, corresponding to the primary alcohol carbon (C6), secondary alcohol carbons (C2–C5), and the anomeric carbon (C1), respectively. The aromatic region, with peaks around 129.5ppm and 133.8ppm, reflects CH carbons from the terephthalate rings in PBAT, while the signal near 164.3 ppm is consistent with ester carbonyls.

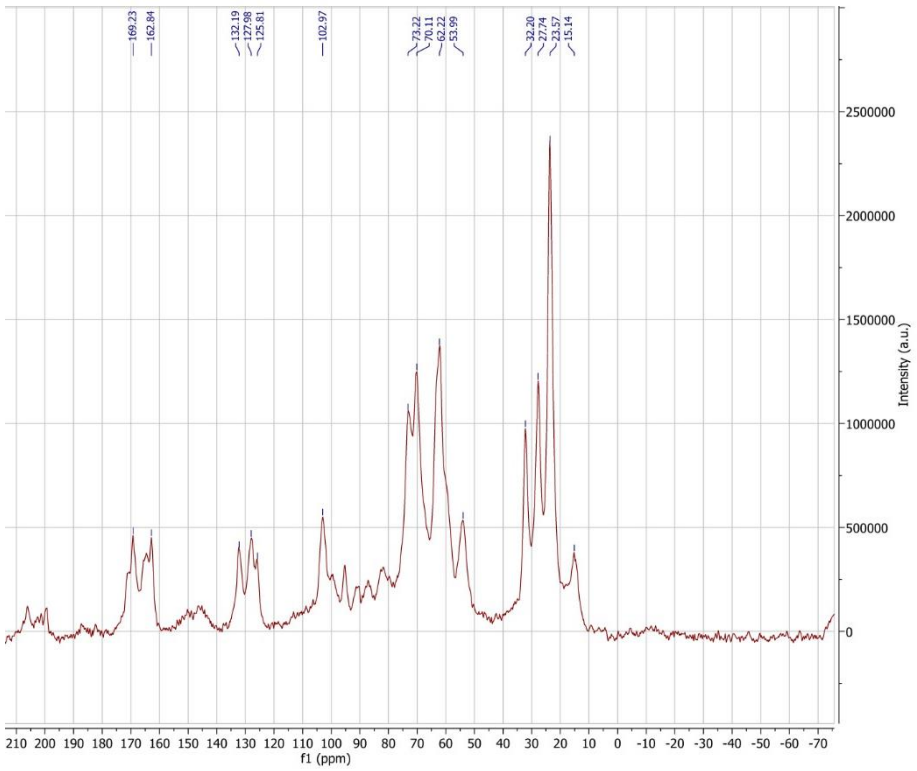

Figure 16. Solid-State ^{13}C NMR Spectra of* PLA + PBAT/PBST + $CaCO_3$ polymer and compost *by measuring Intensity (a.u.) against Chemical Shift (ppm) seen as f1.

Each cluster of peaks can be separated into different functional groups. 15.14ppm to 32.20ppm equates to aliphatic groups, all mentioned in figure 12. The cluster of 53.99ppm to 73.22ppm consists of two peaks expected from the compost part of the sample, the N-alkyl from an amino acid or microbial biomass and an O-alkyl. This Oalkyl peak relating to compost does overlap with the same group found in PLA. The single peak at 102.97ppm is from the anomeric carbon from the compost's polysaccharides, whilst the cluster between 125.81ppm and 132.19ppm are all aromatic carbons from the polymer additives and compost. Finally, the peaks at 162.84ppm and 169.23ppm are carbonyls from PBAT/PBST and PLA respectively, with the PLA carbonyl having a contribution from $CaCO_3$, which typically resonates in the 168-171ppm region (Sen et al., 2016).

4.4.4 Theoretical Polymer and Compost spectra

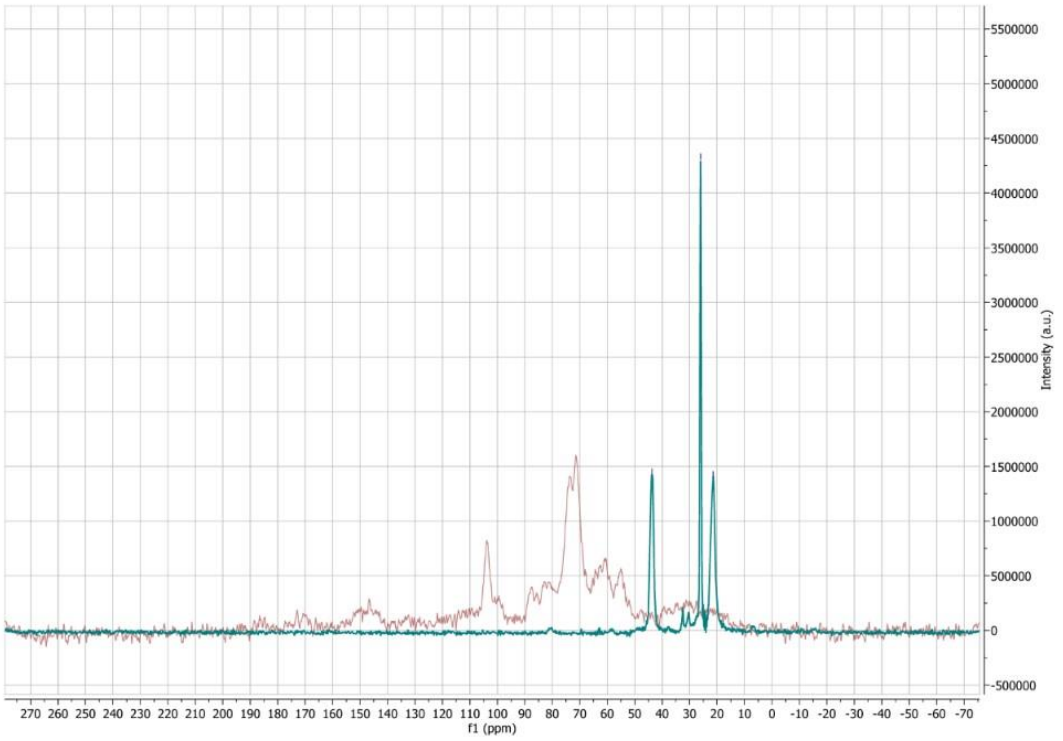

Figure 17. Solid-State 13C NMR Spectra of PP (in blue) superimposed onto the compost sample (red) by measuring Intensity (a.u.) against Chemical Shift (ppm) seen as f1.

The superimposed ^{13}C SSNMR spectra of compost (red) and polypropylene (PP, blue) offer a practical and insightful approach to peak attribution when time or resources prevent the preparation of physical mixtures. In this overlay, the blue spectrum of PP shows sharp, well-defined peaks particularly the intense signal near 30 ppm, which corresponds to the methylene and methyl carbons in the polymer backbone. These peaks are characteristic of PP's semi-crystalline structure and dominate the aliphatic region.

In contrast, the red compost spectrum exhibits broader, less intense signals with a noisier baseline, reflecting the chemically diverse and amorphous nature of organic matter. Peaks in the compost spectrum may arise from carbohydrates, lignin derivatives, humic substances, and microbial metabolites, typically appearing in regions spanning 60–110 ppm and beyond.

By overlaying the two spectra, one can visually isolate which peaks are unique to PP and which are contributed by compost. This comparative

method allows researchers to hypothesize which signals would be retained, suppressed, or shifted in a true mixture. For example, if a peak appears in both spectra at similar chemical shifts, it is likely to persist in the blend. Conversely, if compost signals overlap or obscure polymer peaks, one can anticipate reduced resolution or altered intensity in the mixture.

This technique is especially useful for planning SSNMR experiments, assigning peaks in complex systems, and predicting spectral behaviour without committing to full sample preparation. It provides a rapid, non-destructive way to assess compatibility, interference, and signal dominance—making it a valuable tool in polymer degradation studies and environmental material analysis.

4.5 SSNMR: T1 Relaxation

In the spectra presented above, the resonances from the different polymers are clearly distinguishable from the background signals from the compost, despite there being substantial overlap of the ^{13}C chemical shifts. The ratio of polymer to compost was quite high in the samples described above, however, for samples containing much lower amounts of plastics, it would be more difficult to distinguish the polymer signals when the compost signals dominate the spectrum. A SSNMR approach based on T_1 editing was therefore investigated as a means of reducing or eliminating the signal from the compost, whilst retaining the resonances from the polymer. The experiment exploits differences in the T_1 relaxation times of the polymer and compost nuclear spins; XRF analysis indicates that the compost contains traces of iron and manganese, which exist as paramagnetic ions Fe2+ and Mn2+. Hence, the T_1 relaxation times for ^{13}C nuclei in compost are expected to be shorter than in the polymer. By using an inversion-recovery experiment (see Methods), a recovery delay may be selected at which the ^{13}C signals for the compost are nulled and the signals from the polymer are observed.

Figure 16 shows a series of spectra obtained in an inversion-recovery experiment on compost alone. At the shortest recovery time (spectrum 1 in Figure 16), the signals are inverted, but rapidly recover to become positive, passing through zero in the second spectrum. By contrast, the inversion recovery spectra of PE (Figure 20) require much longer recovery times before the signal passes through the zero point. This is because the T_1 relaxation time of the polymer is longer than for compost. Measurements of the remaining polymers (Figures 21-24) also show

longer T_1 relaxation times compared to that of the compost. Hence, by selecting a short recovery time, the signal from PE can be detected selectively.

Untreated Compost:

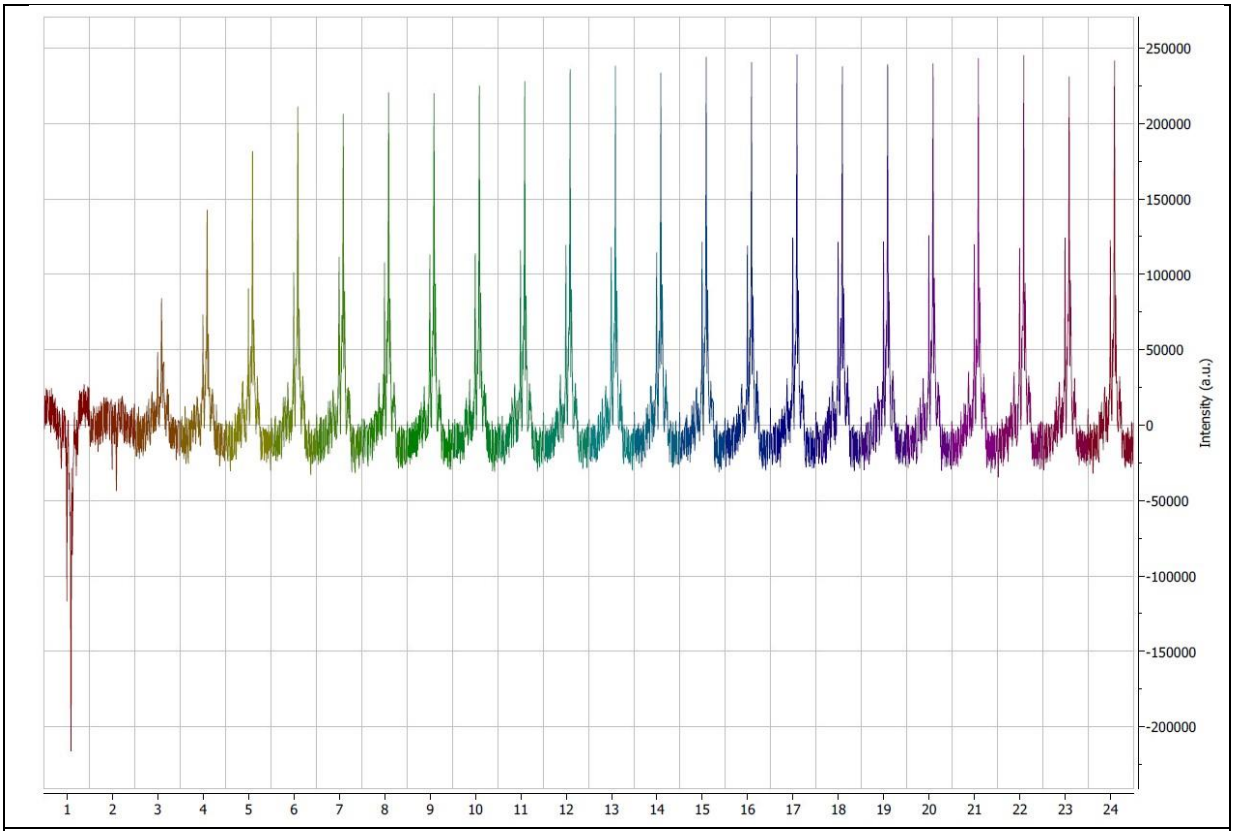

***Figure 18. Solid-State ^{13}C NMR Spectra of* the T1 relaxation of untreated compost *by measuring Intensity (a.u.)*.**

The T_1 relaxation SSNMR spectrum of untreated compost reveals rapid signal buildup and decay across short delay times indicate fast relaxation behaviour, typical of mobile, low-molecular-weight organic compounds and hydrated regions. Compost is composed of a diverse array of materials—such as lignin fragments, cellulose, proteins, and microbial metabolites—each contributing distinct relaxation characteristics. These components tend to exhibit short T_1 values due to their amorphous nature and high molecular flexibility, resulting in broad, low-intensity peaks and a noisy baseline.

PE:

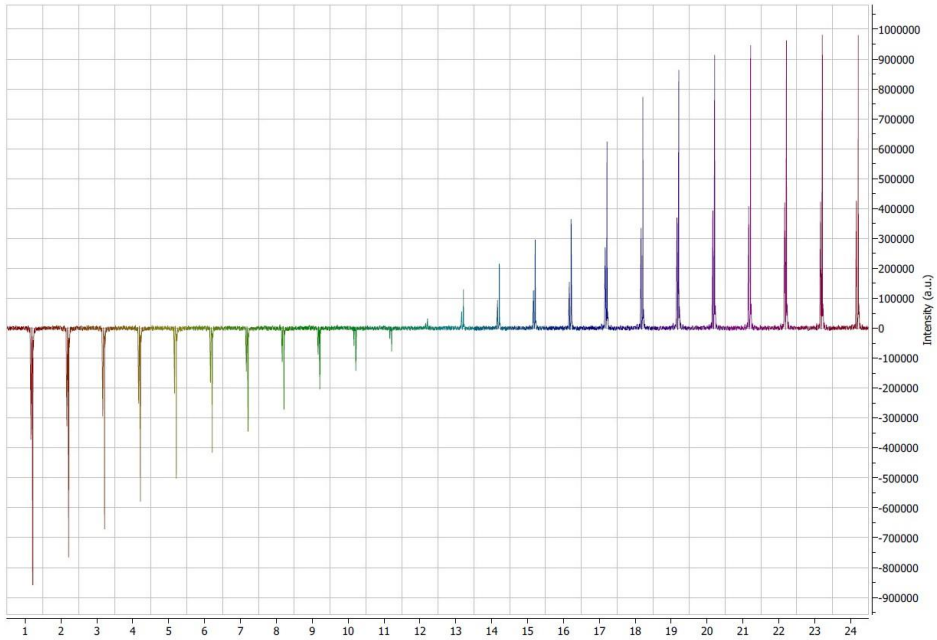

***Figure 19. Solid-State ^{13}C NMR Spectra of* the T1 relaxation of PE by measuring intensity (a.u.).**

Polyethylene (PE) exhibits slower T_1 relaxation times than compost due to its semi-crystalline structure and restricted molecular mobility. In PE, the rigid, repeating $–CH_2–$ units limit energy exchange with the surrounding lattice, resulting in longer spin-lattice relaxation and gradual signal recovery. Compost, by contrast, is composed of mobile, low-molecular-weight organic compounds and hydrated regions that relax rapidly, producing short T_1 values and fast signal buildup. This difference in T_1 can allow an elimination of the compost signal, allowing even tiny amounts of polymer to be isolated and detected.

Pure PLA:

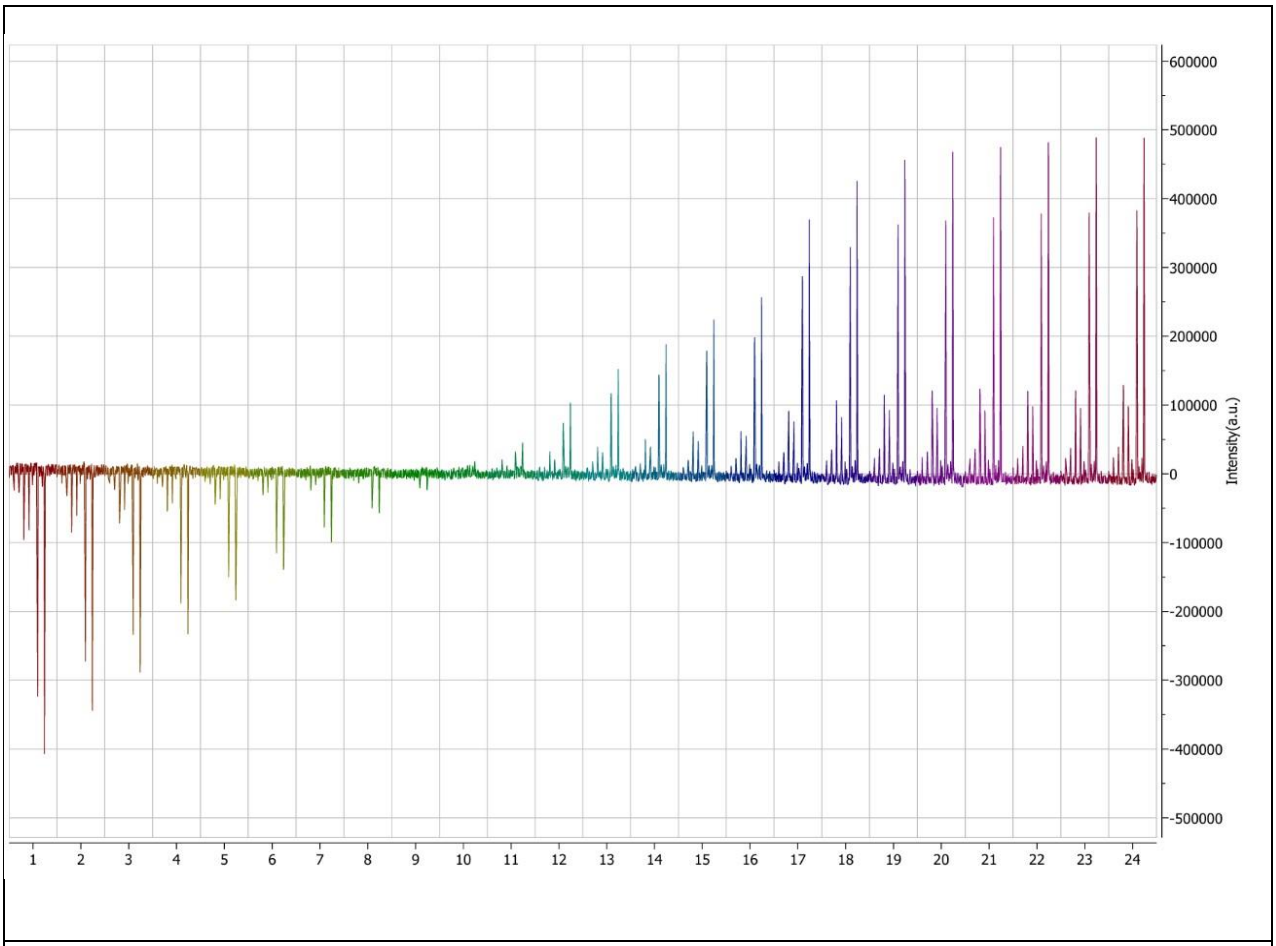

Figure 20. Solid-State ^{13}C NMR Spectra of* the T1 relaxation of Pure PLA *by measuring Intensity (a.u.)

Polylactic acid (PLA) exhibits slightly quicker T_1 relaxation times than polyethylene (PE), primarily due to its more flexible molecular structure and lower crystallinity. PLA's backbone contains ester linkages and asymmetric carbon centers that allow for greater segmental motion, enabling ^{13}C nuclei to relax more rapidly. In contrast, PE's highly ordered $–CH_2–$ chains form a semicrystalline matrix that restricts molecular mobility, resulting in slower energy exchange and longer T_1 values.

Potato Starch (TPS) + PBAT/PBST:

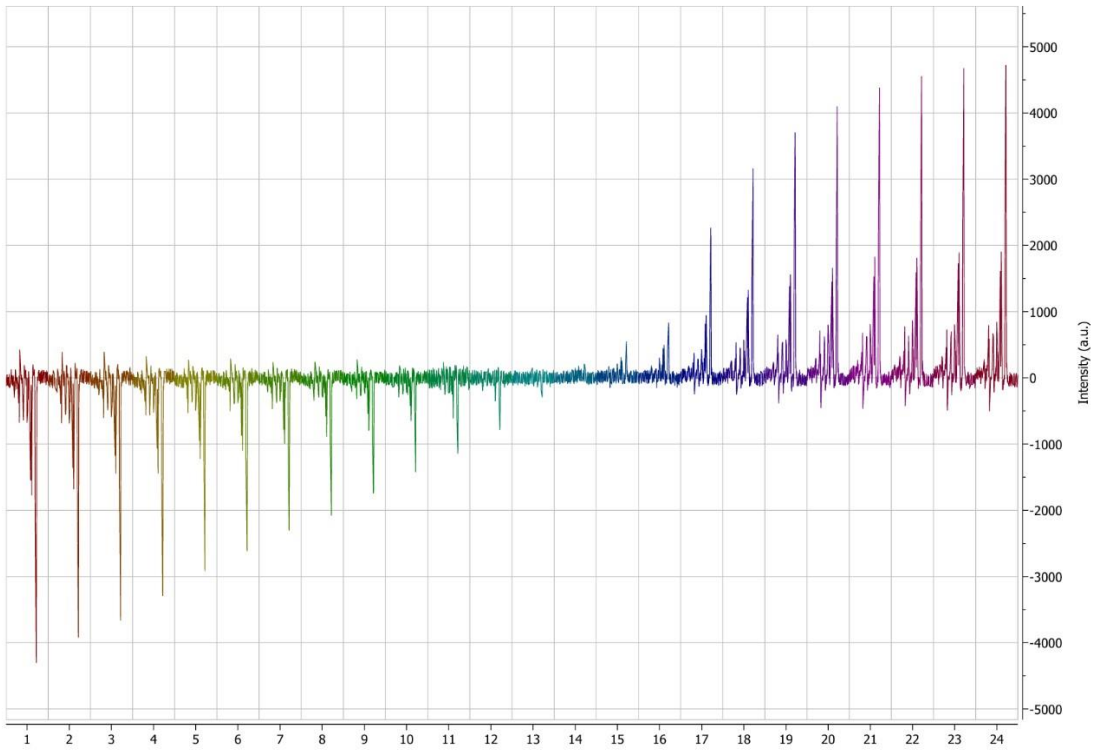

***Figure 21. Solid-State ^{13}C NMR Spectra of* the T1 relaxation of Potato Starch (TPS) + PBAT/PBST polymer *by measuring Intensity (a.u.*).**

Potato starch-based plastics exhibit slower T_1 relaxation times than PLA and PE due to their highly amorphous, hydrogen-rich, and structurally complex nature. Unlike the semi-crystalline backbone of PE or the relatively ordered ester-linked structure of PLA, starch plastics are composed of polysaccharide chains with extensive hydroxyl groups and irregular branching. These features promote strong dipolar interactions and hydrogen bonding, which restrict molecular motion and slow down spin-lattice relaxation.

Corn Starch (TPS) + PBAT/PBST:

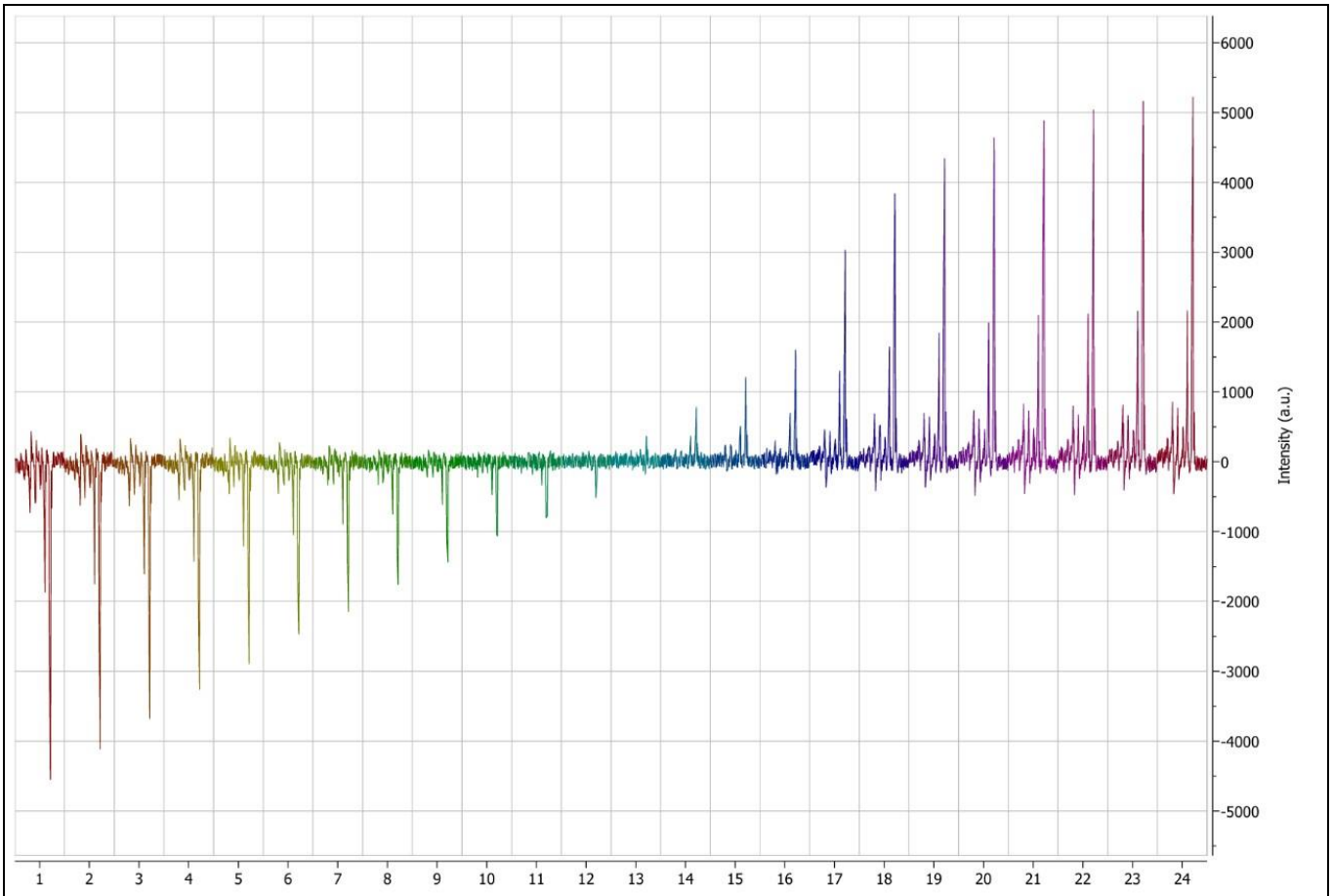

Figure 22. Solid-State ^{13}C NMR Spectra of* the T1 relaxation of Corn Starch (TPS) + PBAT/PBST *by measuring Intensity (a.u.).

Corn starch-based plastics exhibit slower T_1 relaxation times than PLA and PE, similar to potato starch, but with subtle differences in their relaxation behaviour. Corn starch tends to have slightly shorter T_1 values than potato starch, which may be attributed to its more linear amylose content and lower degree of branching. This structural difference allows for marginally greater molecular mobility, resulting in slightly faster spin-lattice relaxation. In contrast, potato starch contains a higher proportion of amylopectin, which introduces more branching and hydrogen bonding, leading to a more rigid matrix and longer T_1 times.

PLA + PBAT/PBST + $CaCO_3$:

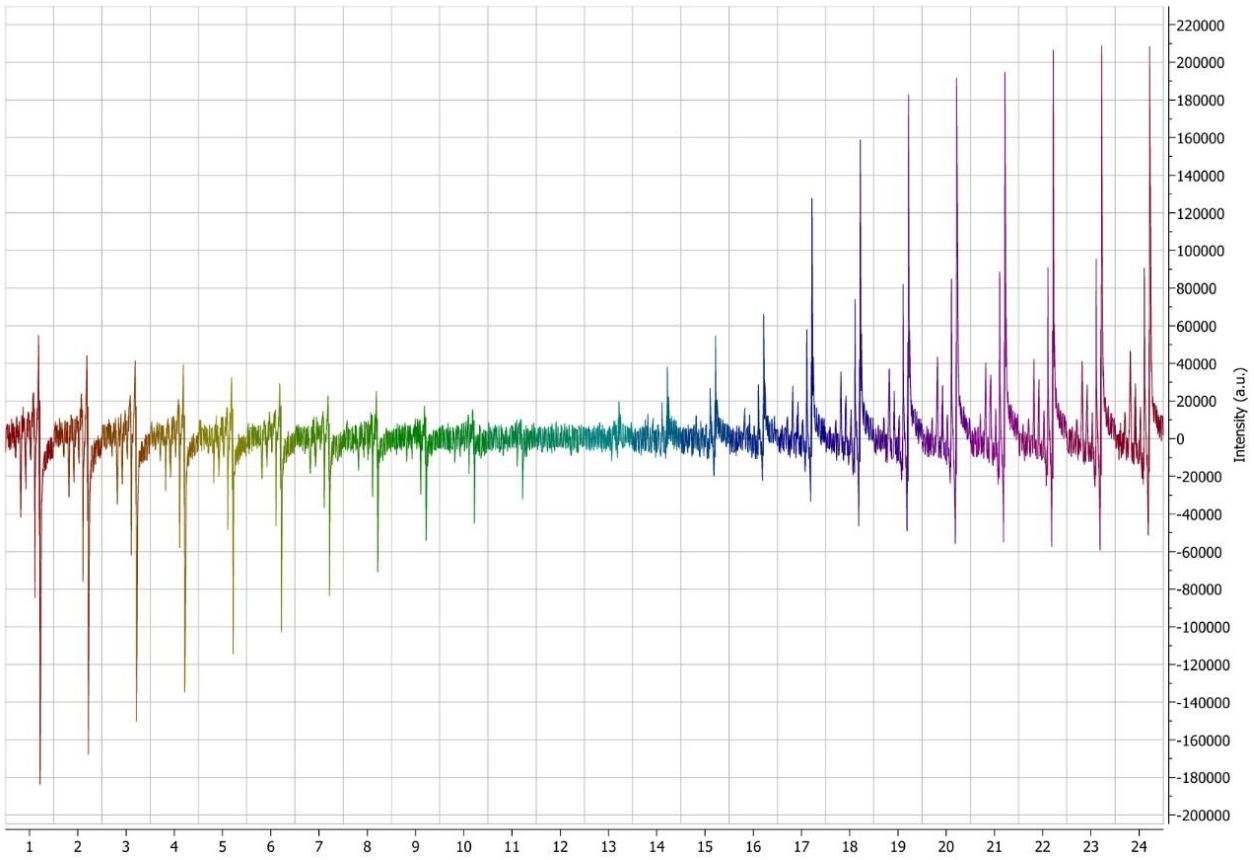

***Figure 23. Solid-State ^{13}C NMR Spectra of* the T1 relaxation of PLA + PBAT/PBST + $CaCO_3$ *by measuring Intensity (a.u.)*.**

Compared to potato and corn starch, the PLA + PBAT/PBST + $CaCO_3$ is more structurally ordered and less hydrated, resulting in shorter T_1 values. PLA contributes slightly faster relaxation due to its more flexible backbone and lower crystallinity, while PBAT/PBST, with its aromatic terephthalate units and longer aliphatic chains, relax more slowly. The presence of $CaCO_3$, although not directly visible in the spectrum due to poor cross-polarization efficiency, contributes to local magnetic field inhomogeneities and subtle peak broadening, further slowing relaxation in nearby polymer segments.

4.6 Changing Polymer to Compost Ratio and Eliminating the Compost signal

Pure PLA and Compost 50:50

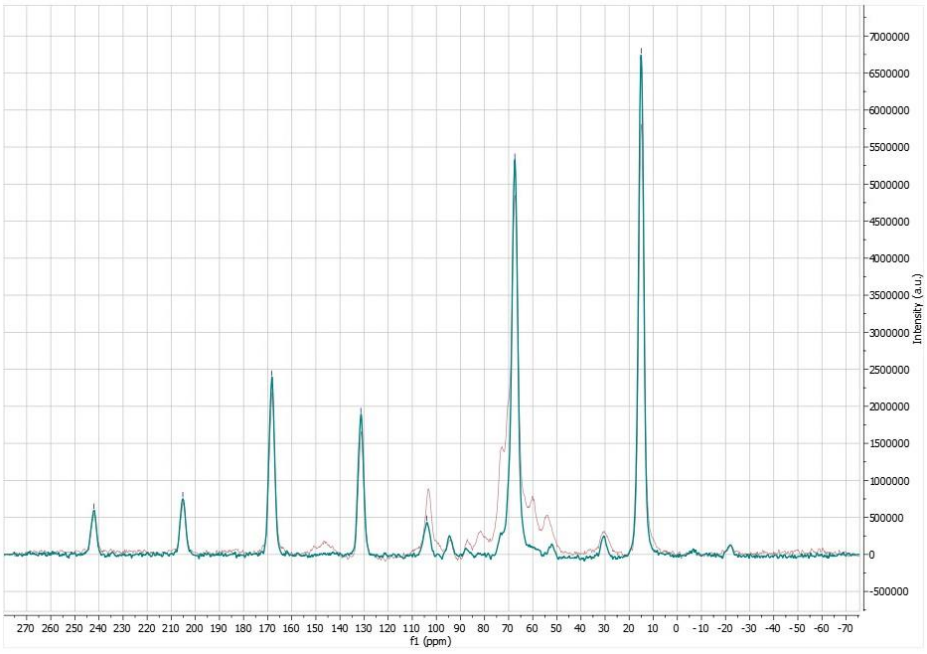

Figure 24. Solid-State ^{13}C NMR Spectra of* Pure PLA and Compost in a 50:50 ratio *with* (red) *and without* (blue) *the compost by measuring Intensity (a.u.) against Chemical Shift (ppm) seen as f1.

The SSNMR spectrum of the 50:50 PLA and compost blend, shown with the red trace representing the full mixture and the blue trace isolating the PLA signal, demonstrates the analytical power of using the difference in T1 relaxation times to remove the compost signal. In the red spectrum, compost contributes a broad, noisy baseline and overlapping peaks, particularly in the 60–110 ppm region. These signals obscure the finer details of the PLA structure, making it difficult to resolve key carbon environments such as the CH group near 69–72 ppm and the ester carbonyl around 170 ppm.

By removing the compost signal (blue trace), the spectrum becomes significantly cleaner and more defined. The sharp peak near 69 ppm, corresponding to the CH carbon adjacent to the ester oxygen in PLA, and the carbonyl cluster around 170 ppm become more prominent and easier to quantify.

Pure PLA and Compost 10:90

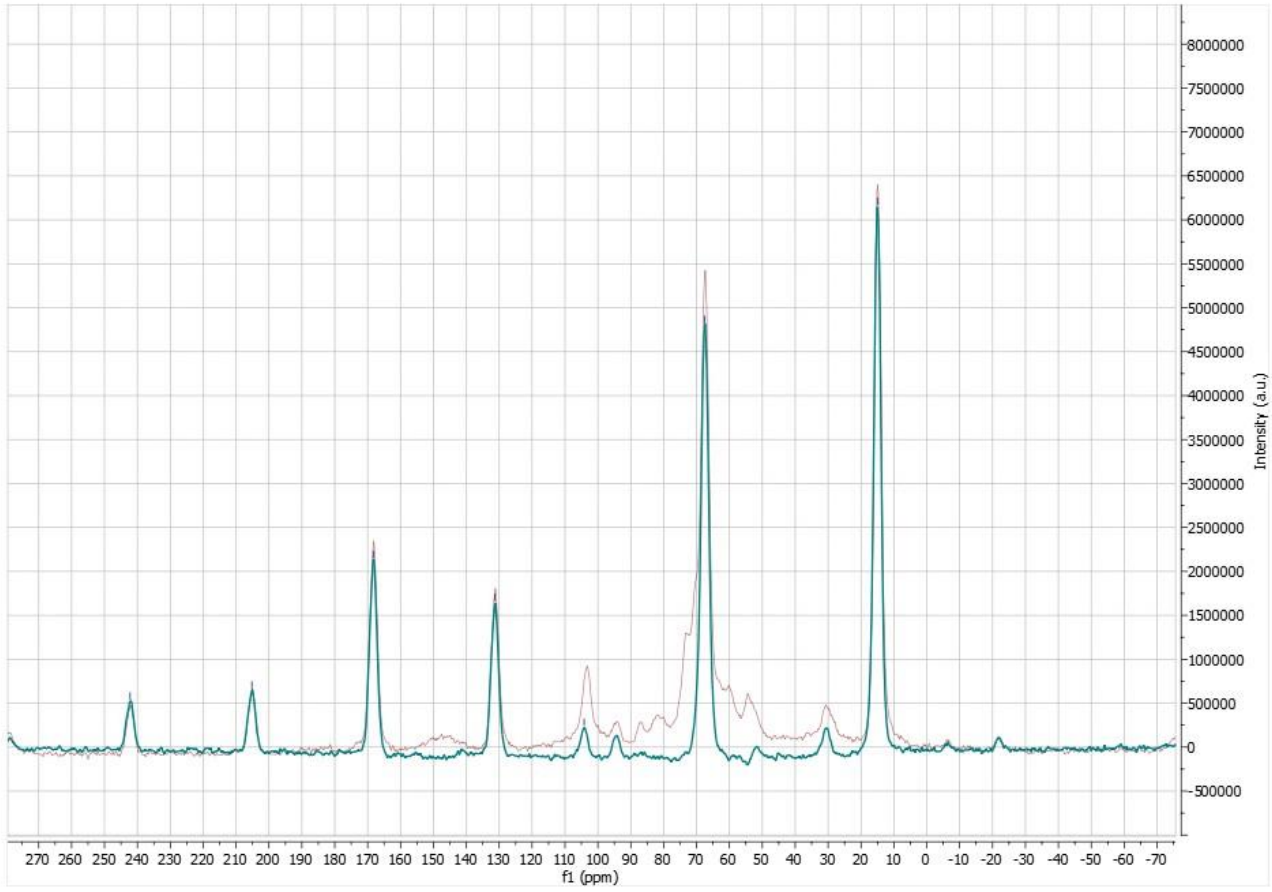

Figure 25. Solid-State ^{13}C NMR Spectra of* Pure PLA and Compost in a 10:90 ratio *with* (red) *and without* (blue) *the compost by measuring Intensity (a.u.) against Chemical Shift (ppm) seen as f1.

Whilst all the PLA peaks are clearly present in the spectra, the change in ratio has affected the intensity of the compost peak, which is to be expected as the amount of compost in the sample increased. However, even with the change in ratio, as all the peaks for PLA are still present, the amount of PLA in the rotor sample can decrease once more.

Pure PLA and Compost 1:99

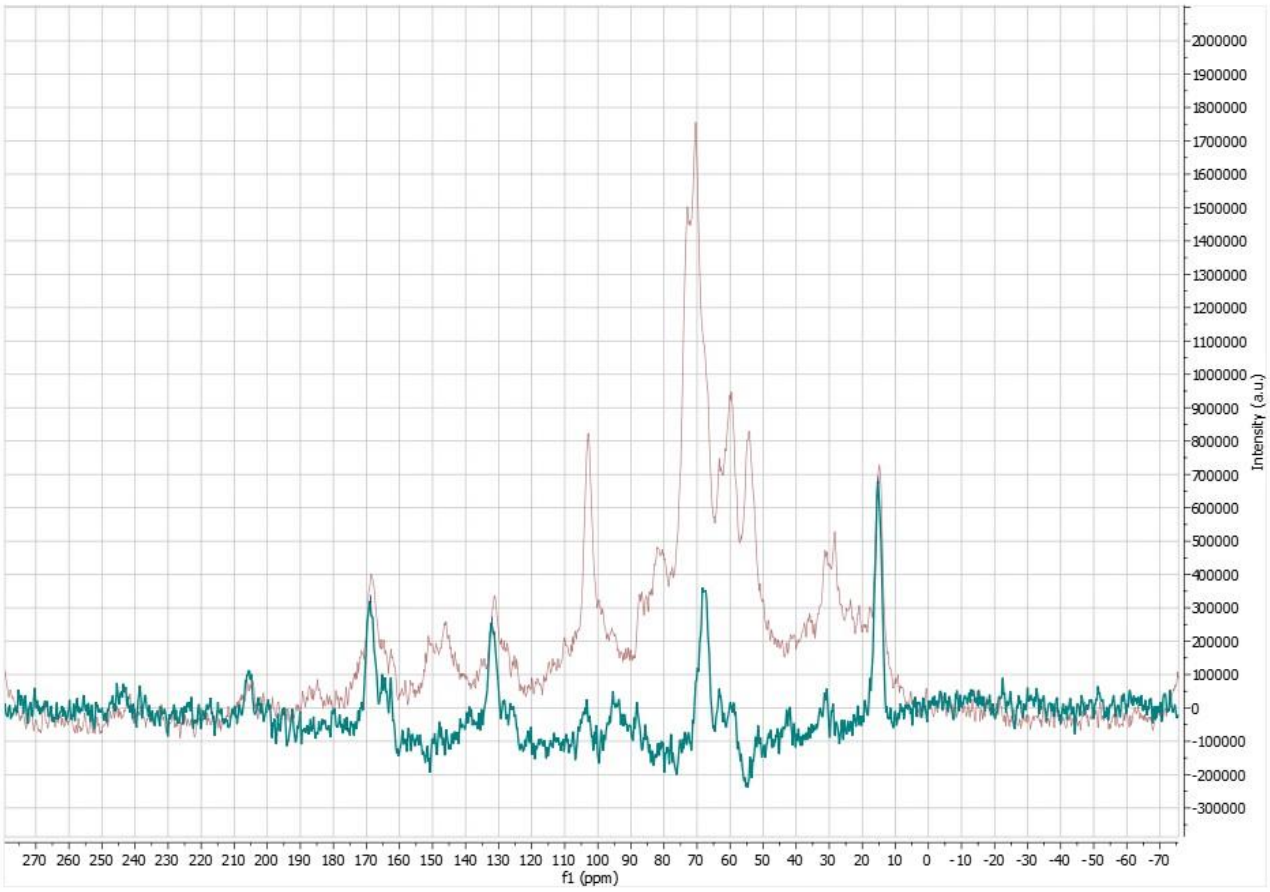

Figure 26. Solid-State ^{13}C NMR Spectra of pure PLA and Compost in a ratio of 1:99 with* (red) *and without* (blue) *the compost by measuring Intensity (a.u.) against Chemical Shift (ppm) seen as f1.

The SSNMR spectrum of the 1:99 PLA : compost blend shows a dramatic shift in signal dominance compared to the 10:90 and 50:50 mixtures. At this extremely low PLA concentration, the compost signal entirely overwhelms the spectrum. Broad, noisy peaks—especially in the 60–110 ppm region—dominate the baseline, reflecting the diverse and mobile organic components of compost. In contrast, PLA's characteristic signals, like the CH resonance near 69–72 ppm and the ester carbonyl cluster around 170 ppm, are barely visible and significantly suppressed.

4.7 SSNMR: Reliability Evaluation

HDPE with Compost

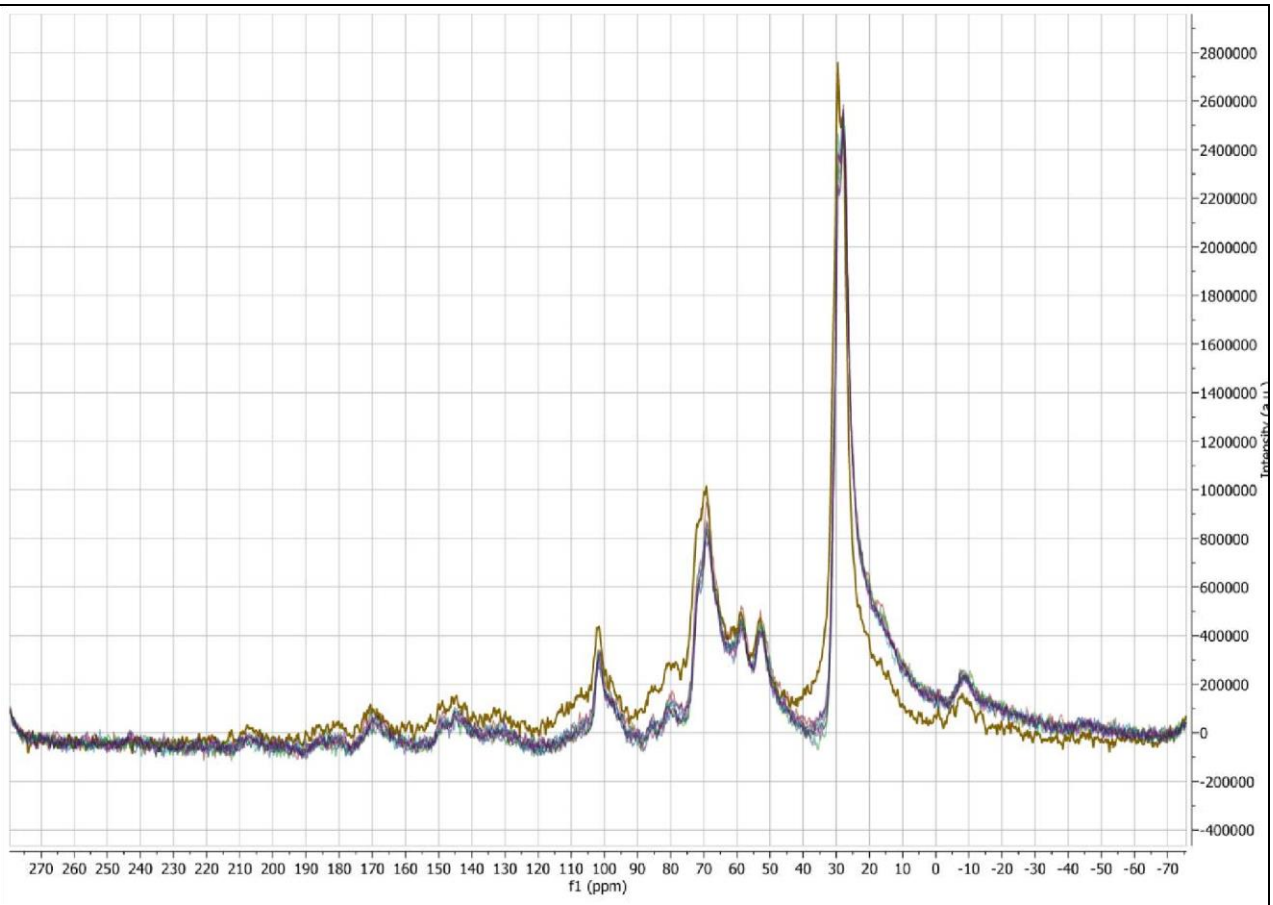

Figure 27. Solid-State ^{13}C NMR Spectra of 10 HDPE and compost spectra superimposed together, measuring Intensity (a.u.) against Chemical Shift (ppm) seen as f1. *Features the same sample of HDPE and compost analysed continuously and spread over 10 sets of results. No settings were changed in between runs and each experiment was ran over 12 hours to add validity to the results and to take out some of the possible variation.*

To test reliability, running the same sample multiple times was a quick and easy method to see the accuracy in the spectra. What ensued was 9 spectra following the same peak structure, with one spectra being an anomaly and shown in bold yellow. Major points to take away are that the peaks themselves are at the same chemical shift but have different intensities than every other spectra.

4.8 SSNMR: Changing Compost pH

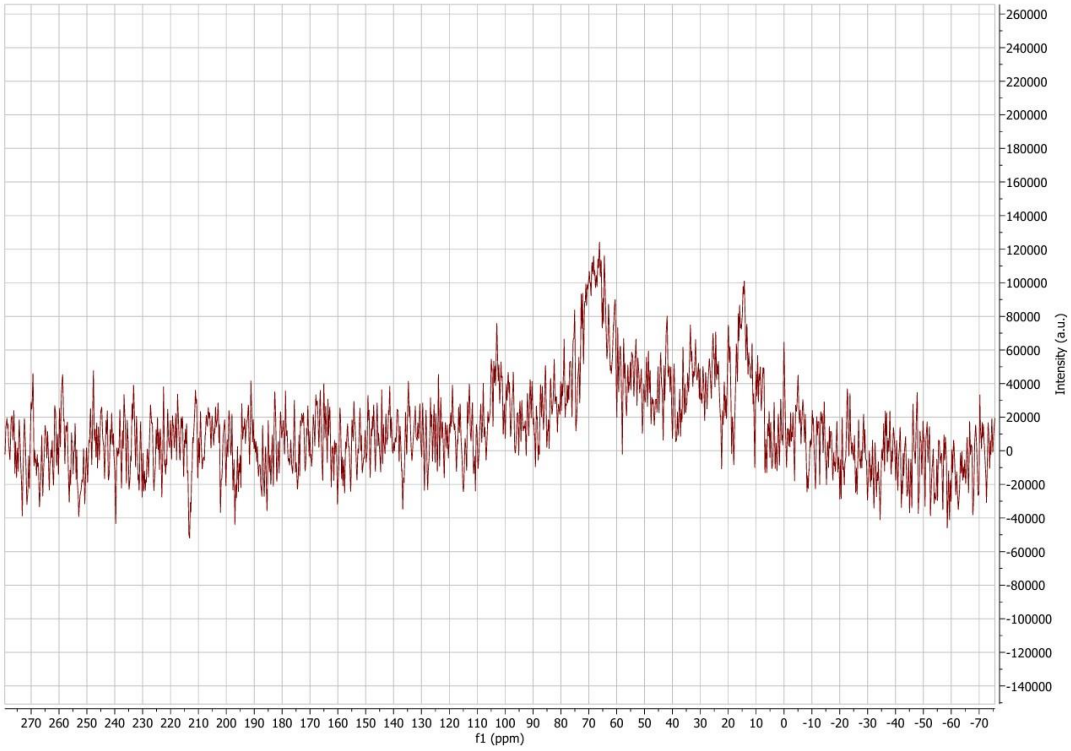

Figure 28. Solid-State ^{13}C NMR Spectra of PLA + PBAT/PBST + $CaCO_3$ with compost changed to pH 14 by NaOH by measuring Intensity (a.u.) against Chemical Shift (ppm) seen as f1.

Figures 28-30 are the result of the method to try and artificially change the pH of the compost to see how compost at different pH levels would change the degradation time of plastics. When samples were made up, if a polymer had broken down due to this pH change before it had time to be examined in the rotor, it would not appear and look like the sample only contained compost instead of a polymer as well.

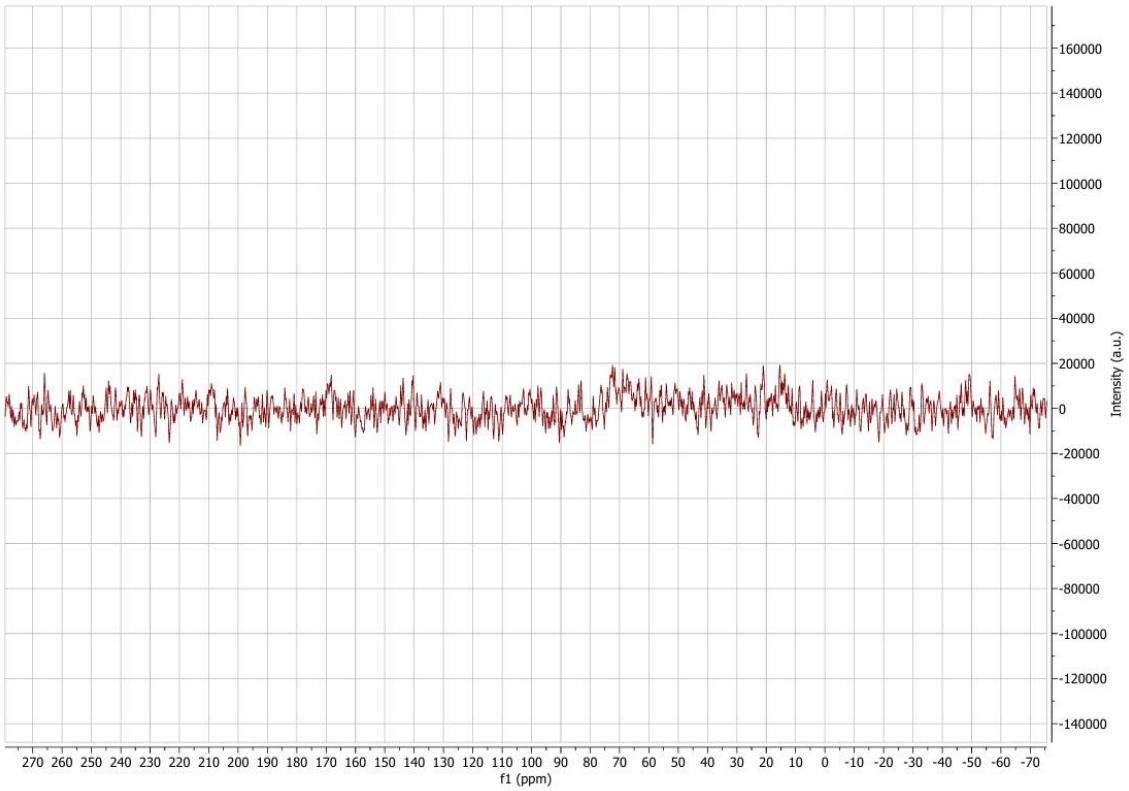

Figure 29. Solid-State ^{13}C NMR Spectra of PLA with compost changed to pH 1 by HCl by measuring Intensity (a.u.) against Chemical Shift (ppm) seen as f1.

The acid-treated compost sample exhibited a flat baseline with significant noise and no discernible peaks, indicating a failure to generate meaningful signal. This result strongly suggests that the sample was damp at the time of acquisition, which can severely compromise spectral quality by disrupting cross-polarization efficiency, accelerating transverse relaxation, and introducing rotor instability during magic angle spinning. Moisture increases molecular mobility, particularly of protons, which interferes with dipolar coupling and suppresses ^{13}C signal intensity. Consequently, the poor signal-to-noise ratio and absence of resolved resonances reflect a chemically and physically compromised sample environment, rendering the spectrum unsuitable for structural interpretation. These findings highlight the critical importance of thorough sample drying prior to SSNMR analysis to ensure reliable data acquisition and meaningful characterization of compost materials.

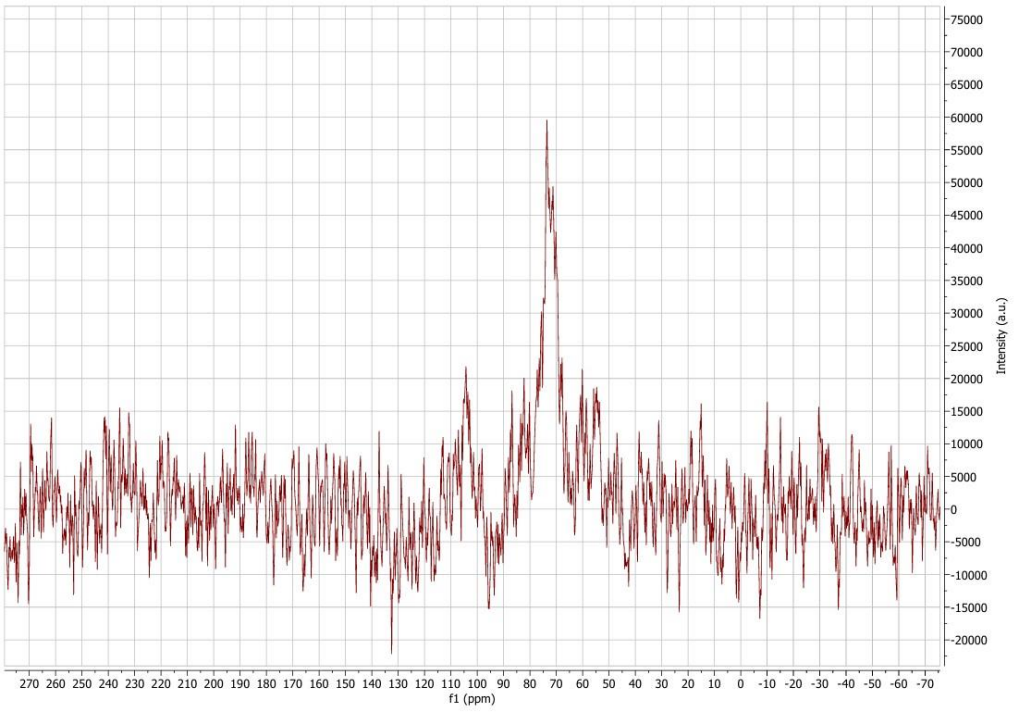

Figure 30. Solid-State ^{13}C NMR Spectra of PLA + PBAT/PBST + $CaCO_3$ with compost changed to pH 14 by NaOH by measuring Intensity (a.u.) against Chemical Shift (ppm) seen as f1.

The pH 14 compost sample containing PLA, PBAT/PBST, and $CaCO_3$ exhibits a prominent resonance centred around 90 ppm, superimposed on a noisy baseline with low overall signal intensity. This peak corresponds to carbonyl carbons from the polyester components (PLA and PBAT/PBST), which are known to resonate in the 160–170 ppm region but may appear shifted or broadened due to the alkaline environment and complex matrix interactions. The high pH, induced by strong base treatment, can lead to partial hydrolysis of ester bonds, increased molecular disorder, and altered relaxation dynamics, all of which contribute to signal broadening and reduced resolution. Additionally, the presence of $CaCO_3$ may influence local magnetic susceptibility and contribute to baseline instability. The emergence of a single dominant peak amidst noise suggests that while some carbon environments remain detectable, the overall spectral quality is compromised—due to a combination of chemical degradation, poor cross-polarization efficiency, and heterogeneous sample packing. These findings underscore the sensitivity of SSNMR to sample pH and matrix composition, and highlight the need for careful control of chemical conditions when analysing compost-polymer systems.

5. Discussion

5.1 Overview

This chapter focuses on the complete evaluation of the study, looking at how the data presented contributes to solving the research aim presented in this thesis. To determine if the technique of SSNMR is a feasible method for detecting plastics and bioplastics in compost, and how well it can detect degradation in these products over time.

The methodology allowed the collection of data showing SSNMR being used for the purpose set out in the aims. Part of the experimental design was focusing on validity over reliability as this is a technique rarely used over other methods like Raman, FTIR or polarised light microscopy (Bläsing & Amelung, 2018). This focus on validity over reliability was taken as it was more beneficial to determine whether the technique was worth pursuing further. This was achieved by changing the ratio of polymer to compost to determine how much polymer had to be in the rotor for accurate detection. Being able to prove that results were possible is more important than knowing if they are repeatable at an early stage in an evaluation. To achieve the required data, a range of experiments were run to ascertain the most credible settings that resulted in the desired outcome.

Due to time and equipment restrictions, spectra was analysed in a more holistic way, as this evaluation is looking at SSNMR on a much broader scale. Reference to specific bioplastics that require their own pieces of research focusing on the feasibility of bioplastics replacing plastics with strong evidence supporting their degradation time and the effects the degraded product has on the environment.

5.2 Differences between compost and polymer spectra

Every polymer individually analysed was shown to have a strong peak between 10ppm and 30ppm that is not present in the untreated compost sample. This peak is the primary source of confirmation that the polymer is present in the compost sample. As polymers will always have a CH_2 or CH_3 bond, unless the polymer is completely cyclised (Winnik, 1985) removing the terminal CH_3, a peak that does not overlap with the compost peak will always be present, adding merit that this technique can be used for a large range of polymers.

Whilst looking into how much a polymer needs to be mixed into the compost in order to detect it, Figure 25 and Figure 26 were simply a

formality as even a ratio of 10:90 polymer to compost proved to be plenty for clear detection. These figures should not be entirely disregarded as they do in the most simplistic way show the power of this technique and provide evidence that results are possible. The nature of how they were produced does limit their application potential as the likelihood of polymer to compost ratios getting to even 10:90 is extremely unlikely. However, Figure 26 provides evidence that even a small quantity of polymer can be detected in compost. Removing the compost and being able to prove that the peak at ~16.00 ppm is undeniable that the polymer is very important, as this peak cannot be mistaken for a compost peak, even with minimal polymer quantity. Being able to remove the compost from the spectra is also an essential component of this technique, as it allows us to superimpose the two spectra to see how much of the spectra is compost and which peaks are identifiable as polymer.

The removal of the compost signal is down to their T1 relaxation times, with Figure 18 showing a much faster relaxation time compared to every other T1 Figure (Figures 19-23). This difference allowed experiments to only collect the readings from the polymer in the rotor, after the compost has been eliminated from the spectra. This technique is a significant component of the analysis, allowing the removal of compost and the detection of whatever remains.

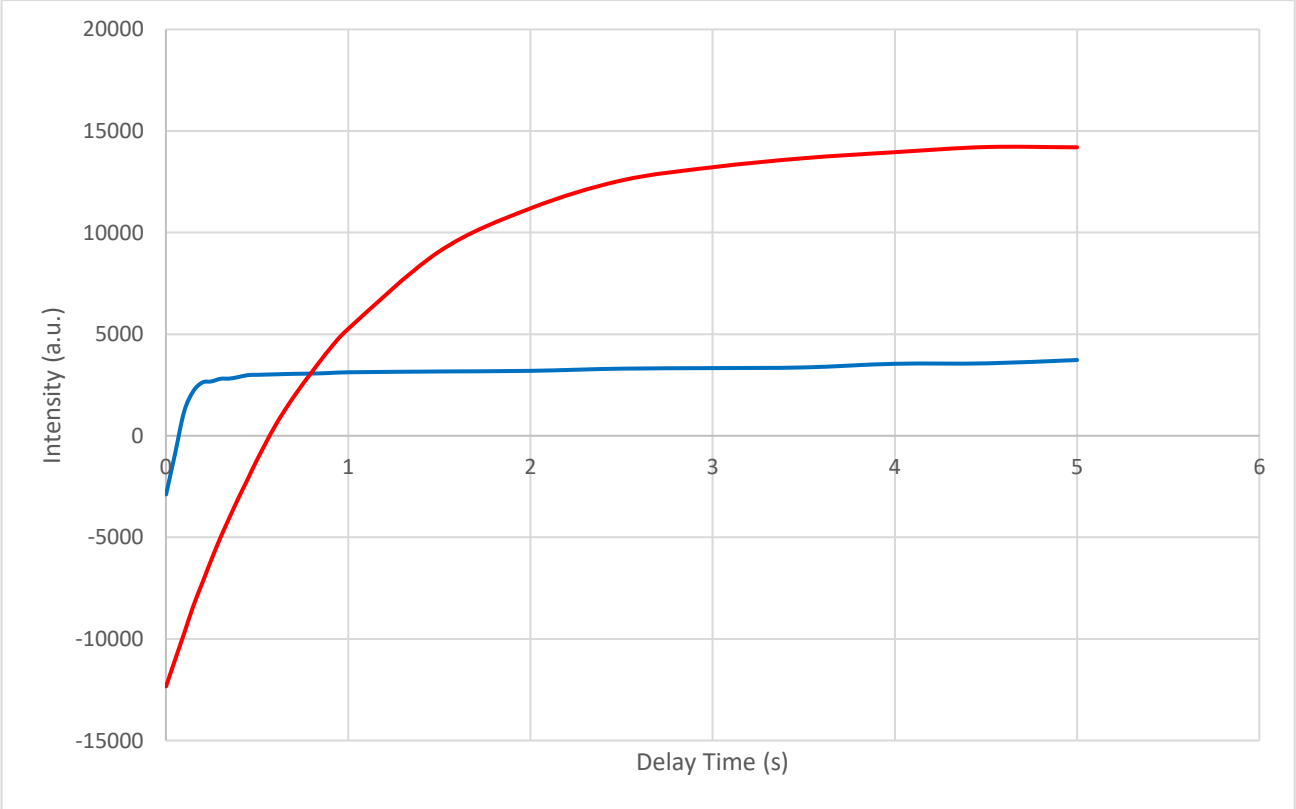

Figure 31. Inversion-Recovery delay curve showing compost (blue) and PE (red)

This difference is exemplified by figure 31, which demonstrates the difference in T_1 relaxation between compost and the polymer PE. Looking and comparing at the delay times between the two, it is clear compost relaxes much quicker, allowing us to have clear distinction between any polymer and compost and therefore being able to eliminate compost when working with smaller amounts of polymer. The composts intensity signal crosses zero at 0.072s, whilst PE crosses zero at 0.571s. This difference is enough to be able to definitively identify what signal is due to compost.

Figure 27 represents reliability by testing the same sample 10 times, one after the other, with a 90% reliability where the spectra was completely identical. The 10% variance had peaks in the same place, with varying intensity. Bonds are identified by their chemical shift, rather than their intensity. A peak requires a certain level of intensity to become a peak but in this case, every peak present in the identical 9 was also present in the other spectra. A concern would be if the chemical shift had changed instead, but as there is evidence that the experiment was not 100% accurate throughout all ten rounds of analysis there is a need to investigate further. This method needs expanding to include the same materials in a new sample instead of using the same sample to make sure the chemical shift does not change with different samples.

Another comparison made was how changing the pH affected the degradation rate. This was to determine whether compost at different pH levels could assist in the degradation of microplastics and if SSNMR could detect any changes in the spectra. Every sample originally used compost samples at pH 7, before being changed using HCl or NaOH to lower or raise the acidity of the compost.

Using FTIR to analyse the polymers in sheet form, a limitation in the technique was discovered as the transmittance reached 0% at strong peaks in both figure 4 and figure 5 at ~2800cm^{-1} to 3000cm^{-1} leading to no distinction between multiple peaks that would feature in the expected spectra. This could simply be down to the sheet provided being too thick, or the high concentration of $CH_,$ CH_2 and CH_3 stretching vibrations causing the instrument baseline to be reached causing this flatline.

The XRF was used to determine the amount of organic matter was present in compost compared to the minerals found. After looking at both humid and dry samples of compost, a humid compost sample was deemed to be ~22.22% water. This causes problems as liquid can

interfere with the signal to noise ratio in SSNMR causing spectra to be much broader and in severe cases, unusable. In spectra C1, this problem is emphasised as despite some essence of individual peaks are present, it is impossible to analyse them at all.

5.3 Limitations

As the experiments were all done in house with the equipment available, the SSNMR was shared with other research groups on a booking when possible, basis. This limited how much analysis could be completed within the time limit. Bioplastics were prioritised, due to their faster degradation rates.

Ensuring rotor packing was consistent was another challenge to overcome. The moisture content of the compost was inconsistent and complicated the packing process. Attempts were made to maintain the humidity levels by using a humidifier, but the moisture still affected the results. This moisture meant compost samples were consistently inconsistent in their packing, whilst the amount was consistent and the packing was done as thoroughly as possible, the packing was not uniform. This affected the stability of the spinning and caused reduced resolution in the spectra.

For an unambiguous evaluation there would need to be a method for ensuring consistent moisture levels and have a more accurate method for packing the material into the rotor, rather than using the inconsistent amount of pressure applied during these experiment.

When investigating how the change in a compost's pH can affect polymer degradation, there was a need to alter the compost pH artificially rather than a naturally in order to first see if this change had any affect. The problem with using chemicals to change composts pH is that it becomes unclear whether the polymer degraded at the higher pH due the compost being a higher pH or simply because it dissolved in the chemical. From additional research, the PLA polymer dissolved in NaOH solution in under 3 hours, this rapid hydrolysis of the polymer does support the idea that if too much NaOH solution was mixed into the compost, it would simply dissolve the polymer instead of working with the compost as a pH increaser.

Another issue with this method is when spinning sidebands can occur as an artefact of magic-angle spinning. These sidebands occur when nuclei experience large chemical shift anisotropy (CSA), where the chemical shift varies strongly with molecular orientation relative to the magnetic field. MAS reduces this anisotropy, but when the CSA is substantial, the averaging is incomplete, producing a series of peaks at integer multiples of the spinning frequency (Mao & Schmidt-Rohr, 2004). This effect is particularly pronounced for carbonyl (C=O) carbons, which possess highly anisotropic electronic environments due to the π-bond and the strong electronegativity of oxygen. As a result, C=O groups routinely generate intense spinning sidebands under typical MAS conditions. In contrast, CH_2 and CH_3 carbons exhibit much smaller CSA values because their electron density is more isotropic and dominated by σ-bonding, and their local motions further average out residual anisotropy. Consequently, CH_2/CH_3 groups produce only very weak sidebands, often below the noise level, and therefore do not contribute visible artefacts in the spectra (Liu & Pruski, 2014). The selective appearance of spinning sidebands from C=O groups is thus fully consistent with their underlying molecular anisotropy and the expected behaviour of MAS-averaged solid-state NMR signals.

5.4 Implications

This research lays the foundations for a long and thorough project into SSNMR as a method of detecting microplastics in compost, as our data shows that both compost and microplastics can both be detected when both present. And if you can eliminate the compost element using the differing T_1 relaxation times, you can isolate the microplastics present. With even a ratio of 1:99 (Plastic to Compost) detection is possible, although as this is all done with manufactured samples that ensure a specific amount of polymer is present in each sample.

From previous literature, we know research has been done into other analytical methods for the concept of detecting microplastics in different environments. However, they primarily focus on oceanic impact using FTIR. Project wants to use SSNMR to detect plastics in compost as if you can detect them, seeing how they degrade over time is a good next step in the development of the research. In being able to do so, plastic production can use this technique to see how degradable their product

is before introducing it as a worldwide product, enabling a new angle to investigate when evaluating a new plastic product.

Could have massive implications in the production of future plastic products as if you can analyse new products specifically with regard to their degradation qualities and how this degradation affects a compost sample could lead to changes in laws for new plastic products requiring to have this analysis complete to confirm it has a quick degradation time and the byproducts created are also not harmful compost samples. As harmful byproducts could leach their way into the compost and potentially end up in the food cycle of humans.

5.5 Future Work

To build upon the findings of this study, several avenues for future investigation are proposed to deepen understanding of polymer degradation in compost environments. First, increasing the number of experiments across multiple samples of identical composition will help assess reproducibility and variability, ensuring that observed trends are statistically robust. Investigating naturally occurring mechanisms for pH alteration—such as microbial activity or organic acid production—may offer more environmentally relevant insights into how pH influences degradation rates. Additionally, varying rotor sizes during SSNMR acquisition could reveal how sample geometry affects spectral resolution and sensitivity, potentially optimizing data quality for complex matrices.

Complementary thermal analysis using Differential Scanning Calorimetry (DSC) to determine polymer melting points, followed by temperaturecontrolled SSNMR experiments, would allow exploration of how thermal transitions influence degradation kinetics and molecular mobility. Another promising direction involves studying the role of plasticdegrading bacteria, with SSNMR used to monitor molecular-level changes as biodegradation progresses. Expanding the range of polymers and biopolymers investigated—including both synthetic and bio-based materials—will enhance the generalizability of the findings and support broader applications in sustainable materials research. One particular biopolymer that is of great interest is polyethylene furanoate (PEF) which is a very new biopolymer and the biodegradable alternative to polyethylene terephthalate (PET).

Finally, collecting compost or soil samples from agricultural sites and analysing them for residual polymer content could provide real-world context for degradation behaviour, helping to bridge laboratory findings with environmental impact. Together, these future directions aim to refine analytical approaches, improve ecological relevance, and support the development of more degradable and sustainable polymer systems.

5.6 Conclusion

This section has explored the effectiveness of Solid-State Nuclear Magnetic Resonance (SSNMR) as a technique for detecting and characterizing polymers within compost environments. Through detailed spectral analysis, it was shown that even low concentrations of polymer—down to a 1:99 ratio—can be confidently identified, with distinct peaks such as those from CH_2 and CH_3 groups providing reliable markers. The ability to distinguish polymer signals from compost is largely attributed to differences in T_1 relaxation times, which allow selective detection and enhance analytical clarity.

Experiments also demonstrated that environmental factors like pH and moisture influence spectral quality and degradation behaviour. While extreme pH conditions posed challenges, moderate adjustments produced interpretable results, reinforcing SSNMR's sensitivity to subtle chemical changes. Additional comparisons with FTIR and XRF highlighted SSNMR's unique strengths in resolving overlapping signals and detecting molecular-level changes in complex matrices.

Overall, the findings affirm SSNMR's potential as a powerful tool for studying polymer biodegradability in realistic compost settings. Its sensitivity, selectivity, and adaptability position it as a valuable method for future environmental and materials research.

6. Conclusion

This study is part of a broader effort to explore new analytical tools for tracking and mitigating microplastic pollution. The urgency of this research cannot be overstated. As global plastic production continues to rise and its environmental impact becomes increasingly evident, the need for reliable, sensitive, and non-destructive methods to detect microplastics in complex matrices such as compost is critical. This work contributes to that growing body of research by evaluating the potential of Solid-State Nuclear Magnetic Resonance (SSNMR) as a viable solution.

The primary aim of this study—to assess the validity of SSNMR for detecting polymers and biopolymers in compost—was successfully achieved. SSNMR proved capable of identifying polymer signals even at low concentrations, with characteristic peaks such as those from CH_2 and CH_3 groups remaining distinguishable from compost background noise. The technique's ability to exploit differences in T_1 relaxation times between compost and polymers enabled selective signal acquisition, enhancing clarity and confidence in peak attribution. This was particularly evident in samples with polymer-to-compost ratios as low as 1:99, where polymer presence was still detectable.

The findings demonstrate that SSNMR is not only a valid method for this application but also a highly useful one. Its sensitivity to molecular rigidity, resistance to spectral overlap, and adaptability to environmental variables such as pH and moisture make it a powerful tool for studying polymer degradation in realistic composting conditions. While complementary techniques like FTIR and XRF offer valuable insights, SSNMR uniquely provides molecular-level resolution in solid, heterogeneous samples—an essential advantage when dealing with environmental matrices.

Given its success in this study, SSNMR clearly warrants further investigation. Future work could expand the range of polymers tested, incorporate naturally sourced compost samples, and explore long-term degradation monitoring. Integrating SSNMR with thermal and microbial analyses would also deepen understanding of degradation mechanisms and environmental interactions.

In conclusion, this research establishes SSNMR as a promising and valid analytical technique for detecting microplastics in compost. It lays the groundwork for future studies aimed at refining detection methods, improving environmental monitoring, and ultimately contributing to the global effort to address plastic pollution through science-driven solutions.

7. References

Alsabri, A., Tahir, F., & Al-Ghamdi, S. G. (2022). Environmental impacts of polypropylene (PP) production and prospects of its recycling in the GCC region. *Materials Today: Proceedings, 56*, 2245–2251. https://doi.org/10.1016/j.matpr.2021.11.574

Bläsing, M., & Amelung, W. (2018). Plastics in soil: Analytical methods and sources. *Science of The Total Environment, 612*, 422–435. https://doi.org/10.1016/j.scitotenv.2017.08.086 (doi.org in Bing)

Bunn, C. W., & Alcock, H. R. (1945). *The crystalline structure of isotactic polypropylene*.

Caba-Flores, M. D., Martínez-Valenzuela, C., Cárdenas-Tueme, M., & CamachoMorales, A. (2023). Micro problems with macro consequences: accumulation of persistent organic pollutants and microplastics in human breast milk and in human milk substitutes. *Environmental Science and Pollution Research, 30*(42), 95139–95154. https://doi.org/10.1007/s11356-023-29182-5

Cantor, K. M., & Watts, P. (2011). 1 - Plastics Materials. In M. Kutz (Ed.), *Applied Plastics Engineering Handbook* (pp. 3–5). William Andrew Publishing. https://doi.org/10.1016/B978-1-4377-3514-7.10001-7 (doi.org in Bing)

Cardoza, L. A., Korir, A. K., Otto, W. H., Wurrey, C. J., & Larive, C. K. (2004). Applications of NMR spectroscopy in environmental science. *Progress in Nuclear Magnetic Resonance Spectroscopy, 45*(3), 209–238. https://doi.org/10.1016/j.pnmrs.2004.06.002 (doi.org in Bing)

Cheng, S. Z. D., & Wunderlich, B. (1986). *Thermal analysis and crystallinity of polypropylene fractions*.

Christian, A. H. (n.d.). *Compost: What Is It and What's It to You*. www.ext.vt.edu

Geyer, R., Jambeck, J. R., & Law, K. L. (2017). Production, use, and fate of all plastics ever made. *Science Advances, 3*(7), e1700782.

Haber-Pohlmeier, S., Stapf, S., van Dusschoten, D., & Pohlmeier, A. (2010). Relaxation in a Natural Soil: Comparison of Relaxometric Imaging, T1–T2 Correlation and Fast-Field Cycling NMR. *The Open Magnetic Resonance Journal, 3*(2), 57–62. https://doi.org/10.2174/1874769801003020057

Hale, R. C., Seeley, M. E., La Guardia, M. J., Mai, L., & Zeng, E. Y. (2020). A Global Perspective on Microplastics. *Journal of Geophysical Research: Oceans, 125*(1). https://doi.org/10.1029/2018JC014719

Jambeck, J. R., Geyer, R., Wilcox, C., Siegler, T. R., Perryman, M., Andrady, A., Narayan, R., & Law, K. L. (2015). Plastic waste inputs from land into the ocean. *Science, 347*(6223), 768–771. https://doi.org/10.1126/science.1260352

Keeler, C., & Maciel, G. E. (2003). Quantitation in the Solid-State 13C NMR

Analysis of Soil and Organic Soil Fractions. *Analytical Chemistry, 75*(10), 2421–2432. https://doi.org/10.1021/ac020679k

Khan, B., Niazi, M. B. K., Samin, G., & Jahan, Z. (2017). Thermoplastic Starch: A Possible Biodegradable Food Packaging Material—A Review. *Journal of Food Process Engineering, 40*(3), e12447. https://doi.org/10.1111/jfpe.12447

Kögel-Knabner, I. (1997). 13C and 15N NMR spectroscopy as a tool in soil organic matter studies. *Geoderma, 80*(3), 243–270. https://doi.org/10.1016/S0016-7061(97)00055-4 (doi.org in Bing)

Liu, S., Guo, J., Liu, X., Yang, R., Wang, H., Sun, Y., Chen, B., & Dong, R. (2023). Detection of various microplastics in placentas, meconium, infant faeces, breastmilk, and infant formula. *Science of The Total Environment, 854*, 158699. https://doi.org/10.1016/j.scitotenv.2022.158699 (doi.org in Bing)

Liu, S.-F., & Pruski, M. (2014). Recent advances in solid-state NMR of polymers. *Progress in Polymer Science, 39*, 1215–1236.

Lorenz, K., Preston, C. M., & Kandeler, E. (2006). Soil organic matter in urban soils: Estimation of elemental carbon by thermal oxidation and characterization of organic matter by solid-state 13C NMR spectroscopy. *Geoderma, 130*(3), 312–323. https://doi.org/10.1016/j.geoderma.2005.02.004 (doi.org in Bing)

Mao, J.-D., & Schmidt-Rohr, K. (2004). Advanced solid-state NMR of natural organic matter. *Solid State Nuclear Magnetic Resonance, 26*, 36–45.

Morrison, O. (2024). Microplastics in soils… how big is the problem? AgTechNavigator. https://www.agtechnavigator.com/Article/2024/01/25/Microplastics-in-soils-how-big-is-the-problem/

Moshood, T. D., Nawanir, G., Mahmud, F., Mohamad, F., Ahmad, M. H., & AbdulGhani, A. (2022). Sustainability of biodegradable plastics: New problem or solution? *Current Research in Green and Sustainable Chemistry, 5*, 100273. https://doi.org/10.1016/j.crgsc.2022.100273 (doi.org in Bing)

Patil, C., Junghare, H., Hamjade, M., Patil, C. K., Girase, S. B., & Lele, M. M. (2020). *A Review on Cryogenic Grinding*. International Journal of Current Engineering and Technology.

Pizzanelli, S., Calucci, L., Forte, C., & Borsacchi, S. (2023). Studies of Organic

Matter in Composting, Vermicomposting, and Anaerobic Digestion by 13C Solid-State NMR Spectroscopy. *Applied Sciences, 13*(5). https://doi.org/10.3390/app13052900

Prata, J. C., da Costa, J. P., Lopes, I., Duarte, A. C., & Rocha-Santos, T. (2020). Environmental exposure to microplastics: An overview on possible human health effects. *Science of The Total Environment, 702*, 134455. https://doi.org/10.1016/j.scitotenv.2019.134455 (doi.org in Bing)

Preston, C. M. (1987). Carbon-13 solid-state NMR of soil organic matter— using the technique effectively. In Baldock & Preston.

Qi, Y., Yang, X., Pelaez, A. M., Huerta Lwanga, E., Beriot, N., Gertsen, H., Garbeva, P., & Geissen, V. (2018). Macro- and microplastics in soil-plant systems. *Science of The Total Environment, 645*, 1048–1056. https://doi.org/10.1016/j.scitotenv.2018.07.229 (doi.org in Bing)

Rani, A. (2024). Types and Sources of Microplastics: A Review. *Journal of Polymer Materials, 39*(1), 17–35. https://doi.org/10.32381/JPM.2022.39.1-2.2 (doi.org in Bing)

Ren, X., Tang, J., Wang, L., & Liu, Q. (2021). Microplastics in soil-plant systems. *Plant and Soil, 462*(1), 561–576. https://doi.org/10.1007/s11104-021-04869-1

Schmidt-Rohr, K., & Spiess, H. W. (1994). *Multidimensional Solid-State NMR and Polymers*. Academic Press.

Sen, S., Kaseman, D. C., Colas, B., Jacob, D. E., & Clark, S. M. (2016). Hydrogen bonding induced distortion of CO_3 units and kinetic stabilization of amorphous calcium carbonate. *Physical Chemistry Chemical Physics, 18*, 21573–21579.

Shi, W., Wu, N., Zhang, Z., Liu, Y., Chen, J., & Li, J. (2024). A global review on microplastics in soils. *Science of The Total Environment, 912*, 169469. https://doi.org/10.1016/j.scitotenv.2023.169469 (doi.org in Bing)

Statista Research Department. (2025). *Global plastic production from 1950 to 2015*. Statista.

Tian, L., Jinjin, C., Ji, R., Ma, Y., & Yu, X. (2022). Microplastics in agricultural soils. *Current Opinion in Environmental Science & Health, 25*, 100311. https://doi.org/10.1016/j.coesh.2021.100311 (doi.org in Bing) Walker, T. R., &

Fequet, L. (2023). Current trends of unsustainable plastic production and micro(nano)plastic pollution. *TrAC Trends in Analytical Chemistry, 160*, 116984. https://doi.org/10.1016/j.trac.2023.116984 (doi.org in Bing)

Wang, Q., & Nielsen, U. G. (2020). Applications of solid-state NMR spectroscopy in environmental science. *Solid State Nuclear Magnetic Resonance, 110*. https://doi.org/10.1016/j.ssnmr.2020.101698

Winnik, M. A. (1985). End-to-end cyclization of polymer chains. *Accounts of Chemical Research, 18*(3), 73–79. https://doi.org/10.1021/ar00111a002

Wirnkor, V. A., Ebere, E. C., & Ngozi, V. E. (2019). Microplastics: A review of analytical techniques. *Analytical Methods in Environmental Chemistry Journal, 2*(2), 13–30. https://doi.org/10.24200/amecj.v2.i2.57

Methods of Calibration Single Point Calibration vs Multiple-point Calibration. (n.d.). https://chem.libretexts.org/@go/page/407714